iTSA
Indian Thermal Spray Association®

June 2022| Vol. 2| Issue 2

SPRAYTODAY™

An INSCIENCEIN publication | Affiliated to the Indian Thermal Spray Association® as its official Newsletter

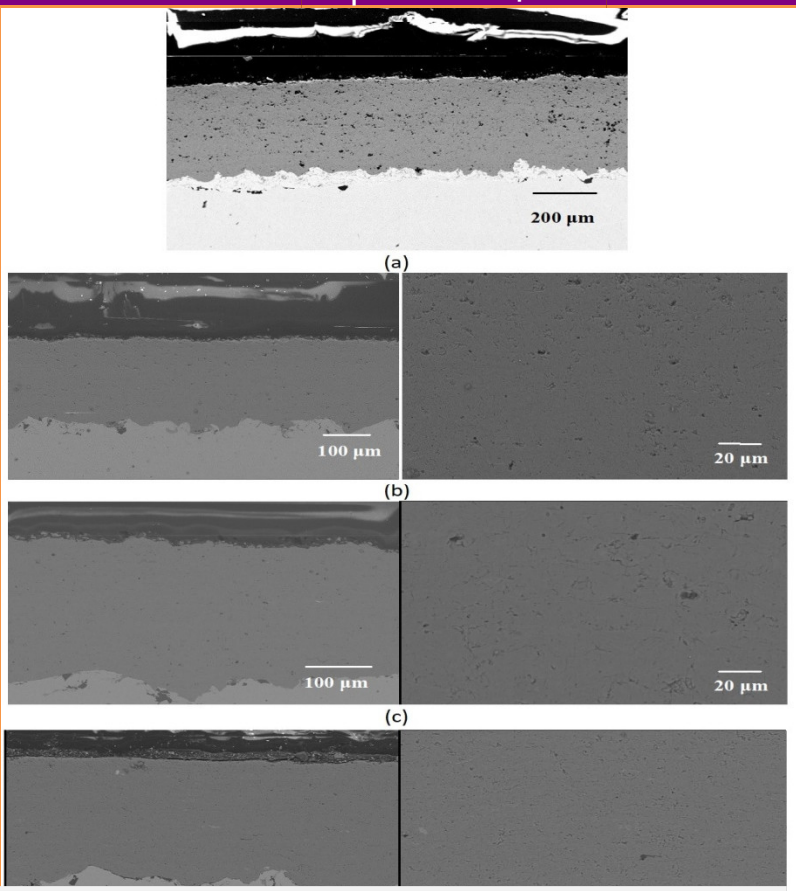

Dense Cr2O3 coating by improved process "H-LVOF"

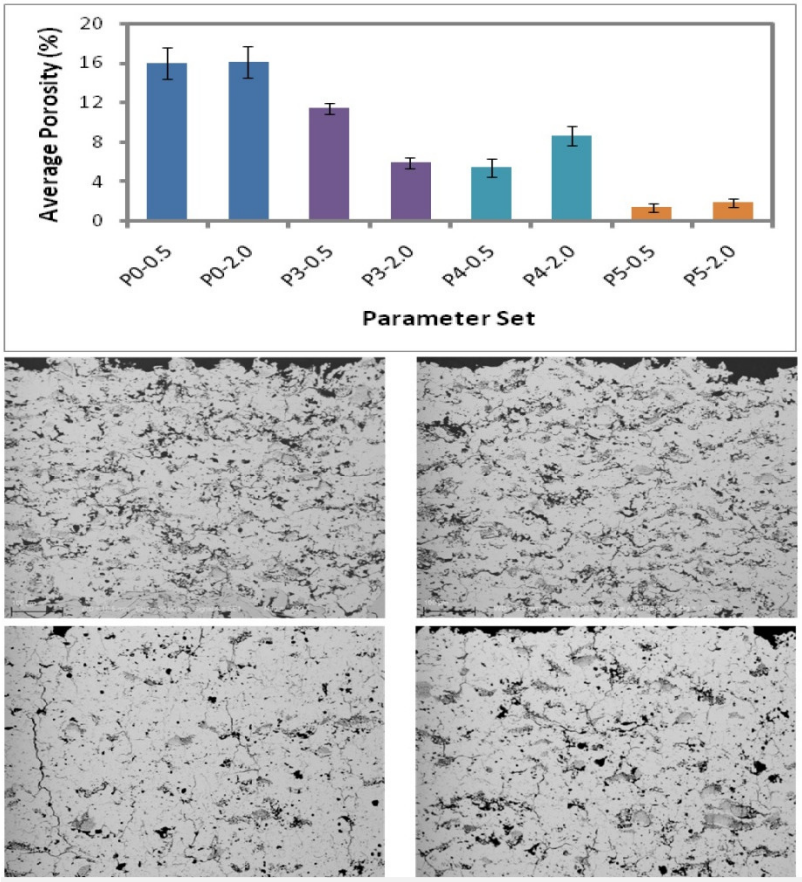

Effect of Target Thickness on TBC Microstructural Features

Issue Highlights

- **Featured Article**: Thermal Spraying Activity at Chemnitz University of Technology
- **Technical Note** : Effect of Target Thickness on the TBC Deposition Characteristics and Microstructural Features
- **Industrial Research**: A Novel Approach to Deposit Dense Cr_2O_3 Coating by Improved Flame Spray Process "H-LVOF"
- **Academia Research**: Structure-Property Correlation and High-Temperature Erosion Performance of Inconel625-Al_2O_3 Plasma-Sprayed Bimodal Composite Coatings
- **Knowledge Point**: Thermal Spray Energy Efficiency Calculations

www.inscience.in/spraytoday

ADVANCED THERMAL SPRAY SYSTEM

PLASMA SPRAY SYSTEM

MASS FLOW CONTROLLED PLASMA SPRAY SYSTEM
Model - AP-2700

AP-2700 FEATURES :-

- Data logging.
- Recipe selection.
- Remote diagnostics.
- Slave / master / manual modes.
- Meet Requirement of Industry 4.0.
- Touch screen mass flow controlled.
- 80kw Standard, 120kw Optional Power Capacity.

MASS FLOW VIEW PLASMA SPRAY SYSTEM
Model - MPS-80

MPS-80 FEATURES :-

- "CE" Approved.
- PLC Controlled.
- Auto & Manual Modes.
- Support 2 Powder Feeder Operation.
- Can Be Integrated With Chiller, Door, External Interlock.

HIGH VELOCITY OXY FUEL SPRAY SYSTEM

Model - AK-2700

AK-2700 FEATURES :-

- Data logging.
- Recipe selection.
- Remote diagnostics.
- Slave / master / manual modes.
- Meet Requirement of Industry 4.0.
- Touch screen mass flow controlled.

XPOJET-5250

XPOJET-5000

MJP-6000

FLAME SPRAY SYSTEM

POWDERJET-86 A

CERAJET GUN
(Patent Applied)

CONTROL PANEL, HV-3100

- Massflow controlled.
- Auto Ignition.
- Built in powder feeder.

MEC
SINCE 1967

METALLIZING EQUIPMENT COMPANY PVT.LTD.
E-101, M.I.A., Phase-II, Basani, Jodhpur - 342005 (India)
Ph: +91 291 2747601 / 2746359
E-mail: marketing@mecpl.com / sales@mecpl.com / biz@mecpl.com
Web: www.mecpl.com

iTSA
Indian Thermal Spray Association®

June 2022| Vol. 2| Issue 2

SPRAYTODAY™

An INSCIENCEIN publication | Affiliated to the Indian Thermal Spray Association® as its official Newsletter

Mission: Our mission is to deliver the most recent thermal spray industry news and keep up to date to thermal spray community by providing company, event, people, product, research, and membership news of interest to industrial leaders, engineers, researchers, scholars, policymakers, and the public thermal spray community.

SPRAYTODAY™ is a quarterly publication of the INSCIENCEIN Publishing, affiliated to the Indian Thermal Spray Association® [iTSA] as its official newsletter. Published and distributed digitally INSCIENCEIN Publishing.
The Indian Thermal Spray Association is a standing committee of the **"ITSA Association for Thermal Spray Technology and Research®", India**.
iTSA and **INSCIENCEIN Publishing** are not responsible for the accuracy of information in the editorial, articles, and advertising sections of this publication. Readers should independently evaluate the accuracy of any statement in the editorial, articles, and advertising sections of this publication that are important to him/her and rely on his/her independent evaluation.

A subscription to **SPRAYTODAY™** is free for individuals interested in the thermal spray and coatings industry.
http://www.inscience.in/spraytoday.html

Contents

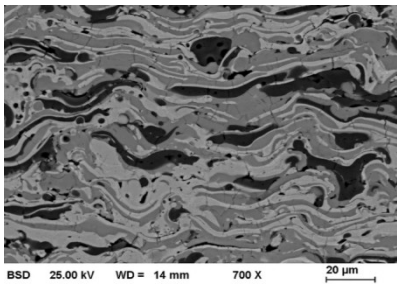

7

Featured Article: **Thermal Spraying Activity at Chemnitz University of Technology**

11

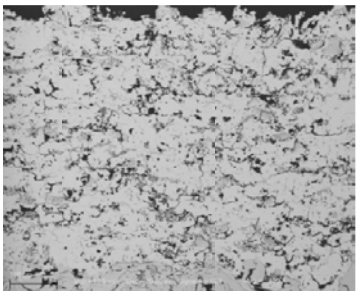

Technical Note: **Effect of Target Thickness on the TBC Deposition Characteristics and Microstructural Features**

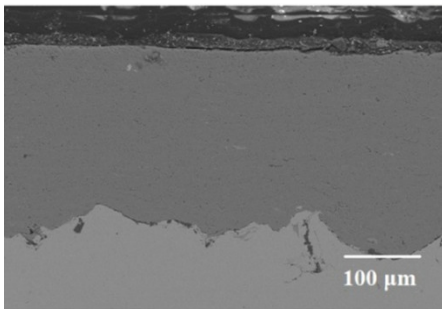

18

Industrial: **A novel approach to deposit dense Cr_2O_3 coating by improved flame spray process "H-LVOF"**

iTSA
Indian Thermal Spray Association®

June 2022| Vol. 2| Issue 2

SPRAYTODAY™

An INSCIENCEIN publication | Affiliated to the Indian Thermal Spray Association® as its official Newsletter

PhD, Postdoc & Research Engineer Job Alerts 15

22

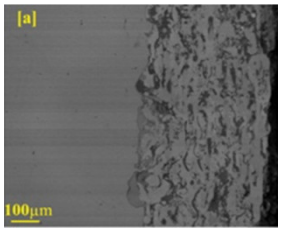

Academic Research: **Structure-property correlation and high-temperature erosion performance of Inconel625-Al_2O_3 plasma-sprayed bimodal composite coatings**

Knowledge Point: Thermal Spray Energy Efficiency Calculations 27

Indian Thermal Spray Asso. Membership 29

Official Journal Publication of the iTSA 29

To contribute an article, advertisement, subscription request, back issue copies, and changes of address should be sent to: todayspray@outlook.com and todayspray@gmail.com

ABOUT THE COVER

Dense Cr_2O_3 coating and TBC Deposition Characteristics

Editor's Note

Dear Readers,

Since the COVID-19 pandemic impacted the world from start of the year 2020, the disease has spread about every country around the world. The Thermal Spray market has experienced negative growth during the pandemic time; however it is expected to be back on track in end of 2022 with resumption of the economic activities.

Asia-Pacific Thermal Spray Market is expected to expand at a projected CAGR of almost 10% during the forecast period, 2022 to 2026. The thermal spray equipment and coating market in India is driven primarily with the increased use of thermal spray coatings in the aerospace, green energy like fuel cell & hydrogen production and nuclear sectors which have grown significantly in the last few years with advancements in technology and R&D, supported by the government.

Due to the global conditions all the major companies are investing in India for their future projects which will definitely increase the thermal spray market in the country.

I am particularly pleased to be allowed to recommend to you the latest issue of the **SPRAYTODAY**. This issue includes invited innovative featured articles from industry and academia experts on the Thermal Spraying Activity at Chemnitz University of Technology, Effect of Target Thickness on the TBC Deposition Characteristics and Microstructural Features, A Novel Approach to Deposit Dense Cr_2O_3 Coating by Improved Flame Spray Process "H-LVOF", Structure-Property Correlation and High-Temperature Erosion Performance of Inconel625-Al_2O_3 Plasma-Sprayed Bimodal Composite Coatings and Thermal Spray Energy Efficiency Calculations, that illustrate current research trends in thermal spray development.

Looking at the future of thermal spray in India, it will be pleasing if **SPRAYTODAY** can also inspire the spirit of thermal spray research in the country by providing the latest information on thermal spray technology.

Be healthy, active and curious.

Best Regards,

(Dr. Satish Tailor)

Kymera INTERNATIONAL
Pioneers in Material Science®

ADVANCED METALLIC COMPOSITE NIOBIUM CARBIDE CLADDING

US Patent Application No: 63/248,885 (patent pending)

Composite Cored Wire Cladding Containing Hard Niobium Carbide

Key Features of this New Innovative Cladding

- Corrosion & erosion resistant
- Non-permeable with treatment
- Cladding easily measurable - Ni base
- High bond strength: > 4000 psi
- Easily repairable
- Porosity: < 4%
- Total oxide content: < 3%
- Hardness: average 56 HRC
- Deposition efficiency: ≈ 68%
- Cladding thickness typically between 6 mils to 125 mils

20% more erosion resistant than other competitor products

Extend service life by **20%**

12x better (sulfidation resistant) than uncoated carbon steel

Innovative Wire Feed Stock

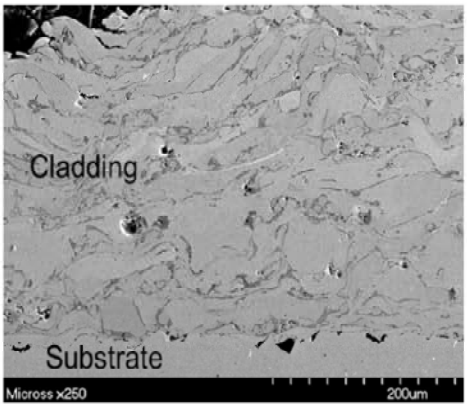

LESS WEIGHT LOSS - BETTER EROSION RESISTANCE

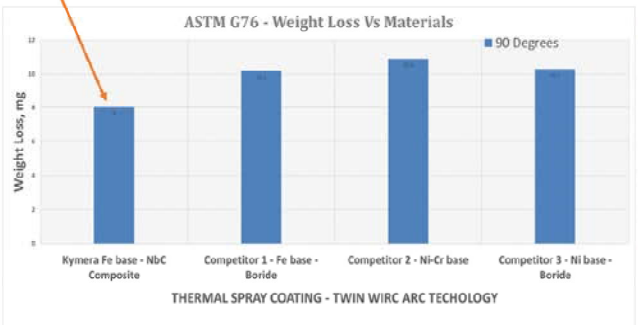

20% MORE EROSION RESISTANT THAN COMPETITOR PRODUCTS IN THE MARKET

NC100 CLADDING - EROSION RESISTANCE	
DISTANCE	10 MM
ORIENTATION	90 DEGREES
VELOCITY	30 M/S
PRESSURE	8 PSI
SCFH	15
MEDIA	ALUMINA ANGULAR SHAPE, 50 µm

Email: info@kymerainternational.com
Web: www.kymerainternational.com
Phone: +1 919.544.8090

Thermal Spraying Activity at Chemnitz University of Technology

*By **T. Lampke, L. Pawlowski,** Institute of Materials Science and Engineering, Materials and Surface Engineering Group, Chemnitz University of Technology, D-09107 Chemnitz, Germany*
Email: lech.pawlowski@unilim.fr

Abstract
The activity in the field of thermal spray of the Institute of Materials Science and Engineering at the Chemnitz University of Technology (CUT) in Germany is briefly reviewed. The involved researchers as well as its organization and the equipment available are described. The examples of research activity are presented as well as that of international collaboration with other groups active in the field.

Creation of laboratory

The activity of thermal spray field in the CUT has started in 1994 by the nomination of Prof. B. Wielage to the Chair of Composite Materials at the Faculty of Mechanical Engineering. The chair holder had an industrial experience and got his PhD in the well-known laboratory of Prof. H.-D. Steffe [1] at the Dortmund University of Technology. Nowadays, thermal spray activity is doneat the Chair of Materials and Surface Engineering managed by Prof. T. Lampke. At present, his group comprises 42 scientific and technical staff and conducts research at the highest scientific level. The core topics of research are:

- Electrolyte development for alloy deposition and conversion coatings;
- New material properties through generative manufacturing and combination processes;
- Design of interfaces and transition structures in hybrid composites;
- Thermomechanical and thermochemical material treatment;
- Material fatigue and damage behavior, especially on coated and corroded materials.

Organization and equipment related to thermal spraying

The thermal spray laboratory, managed by Dr. T. Lindner, is well-equipped enabling development of entire coatings technology starting from powders production up to the sprayed coatings characterization.

The manufacturing of powders is possible using high-energy or planetary ball mills of different types. The mills may work in air, inert gas and vacuum enabling powders of metals, alloys, nanostructured composite powders, such as e.g. FeCrB with CrB2shown in Fig. 1and many others to be developed and produced in the quantities useful for research and development.

The coatings can be thermally sprayed onto the substrates of metals, ceramics, polymers, glasses but also on organic natural materials such as woods, composites. Thermal spray installations are robotized and include among others: (i) atmospheric plasma spraying (APS) with F6 plasma torch of GTV; (ii) high velocity oxy-fuel (HVOF) spraying using powder and wire installations including e.g. TAFA JP5000 set up; and (iii) cold gas spraying (CGS) installation including torch of type Kinetics 3000 of CGT. The thermal spray processes can be optimized using emission spectrometers enabling chemical analysis of species present in flames and jets and the measurements of sprayed particles temperature and velocities during their trajectories in plasma or flame using SprayWatch setup of Oseir. The obtained coatings can be densified by post-spray treatment using e.g. high temperature furnaces or with spark plasma sintering (SPS) applied recently to densify coating of Hadfield steel [2].

The obtained coatings microstructure can be tested using different optical and electron microscopes. The latter includes transmission electron microscope (TEM) of type Hitachi and scanning electron microscopes (SEM) including field emission one of type NEON40EsB equipped in electron dispersive X-ray spectroscopy (EDS) and electron backscatter diffraction (EBSD) setups. The laboratory is also equipped to carry out the tests of: (i) mechanical properties including wear resistance and adhesion of coatings; (ii) corrosion tests at different boundary conditions, e.g. temperature, electrolyte, humidity; and (iii) thermal analyses.

[1] Prof. H.-D. Steffens was an Inductee in Thermal Spraying Hall of Fame in 2002

Research activity

The research activities of the group have started in the 2000-ties with preparation of metal matrix composite (MMC) powders. The composites such as shown in Fig. 1 were sprayed using APS and HVOF techniques and their mechanical properties were characterized and e.g. Vickers hardness tested with 3 N was equal to HV3=1000 and could be useful for paper industry applications. [1].

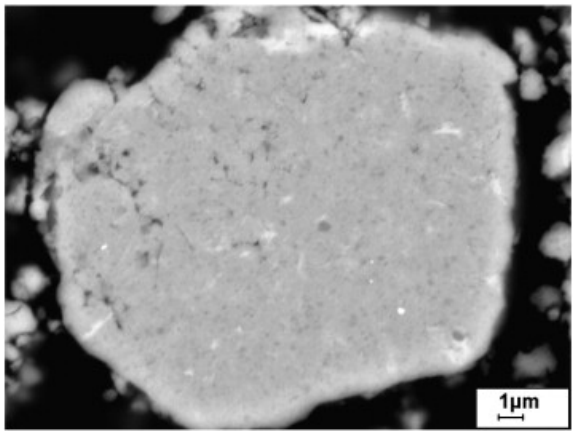

Figure 1: SEM (secondary electrons) of the cross-section of a particle FeCrB+CrB_2 powder produced by high energy milling [1].

The plasma sprayed Fe/TiC wear resistant composite coatings sprayed using powders prepared by self-propagating high temperature synthesis (SHS) weredescribed by Steinhäuseret al. [3]. Similar composites with TiC reinforcement and FeCr matrix were plasma sprayed and CO2 laser glazed to reduce their porosity (see Fig. 2). The microstructure of MMC composed of Al+50 wt.% SiC obtained by HVOF spraying and laser shock treatment was studied using TEM presented by Podlesak et al. [5].

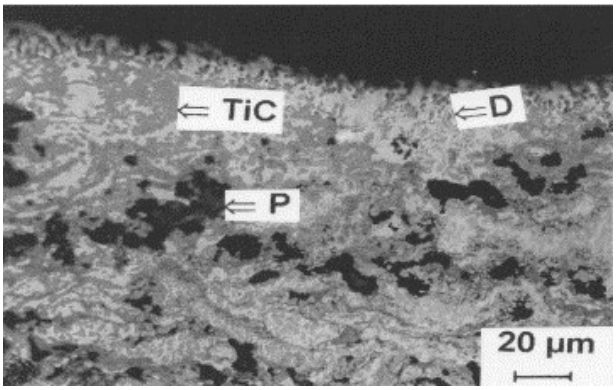

Figure 2: Optical micrograph of polished cross-section of FeCr-TiC coating obtained by plasma spraying and laser glazing. The symbols mean: TiC – grains of TiC reinforcement, P – pore and D – dendrite [4].

The possible applications of the metal coatings of Al and Cu obtained using cold spray onto alumina substrates for power electronic circuits were studied and themicrostructure of and bonding mechanism obtained coatings were analyzed, too [6-8]. Another important industrial application of thermally sprayed coating concerned thermal barrier coatings (TBC). The studies of suspension plasma spraying (SPS) zirconia were carried out to develop columnar microstructure [9-10]. The development of thermally grown oxide (TGO) being an important part of modern TBC starting from a physically vapor deposited (PVD) Al film was studied by Ali et al.[11-12].

Many studies were devoted to understand and to improve the adhesion of coatings to the different type of substrates, and to use the coatings to improve the contact between different types of materials. Consequently, Lindner et al. [13] used arc sprayed wires of NiAl and NiCr alloys to improve the contact between low carbon steel and fiber reinforced polymer layers. Saborowski et al. [14] studied additional methods of enhancing the adhesion between the polymers and metals including grit blasting and laser structuring.

More recently, an interesting idea of plasma spraying of the mixtures of ceramic powders of Al203, Cr203 and TiO2 to obtain the coatings having mechanical properties modified by the content of ternary blend was developed by Grimm et al. [15, 16]. The coatings have the microstructure including lamellas of each oxide, as shown in Fig. 3.

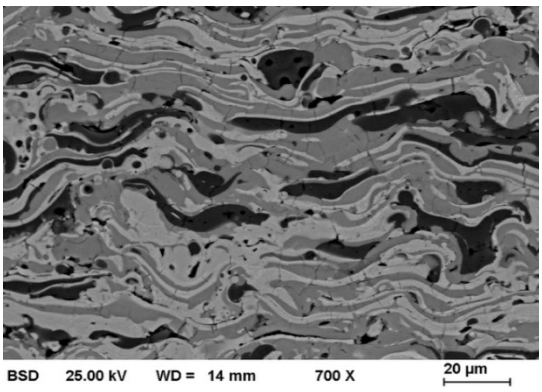

Figure 3: SEM (back scattered electrons) of the cross-section plasma sprayed blend of three oxides. The dark grey lamellas correspond to Al203, medium grey lamellas – to TiO2/TiOx and, the light grey to Cr203 [15].

The most recent study develops the new ideas coming from artificial intelligence modelling methods enabling the remote control of plasma spraying processes [17]. The authors used a so-called fuzzy modelling to predict the cathode wear at APS processes by in-line process diagnostic correlated with the cognition of an operator.

International cooperation and collaboration

The activity of thermal spraying group has been realized in international collaboration with many laboratories. The French-German Laser Center in Arcueil helped in the initial works on laser treatment of sprayed coatings [4-5]. The cooperation in the field of suspension plasma sprayed coatings occurred with the laboratories at: (i) Ecole Nationale Supérieure de Chimie de Lille (France); and, (ii)Wrocław University of Technology (Poland) [9, 10].Finally, the research on TBCs was carried out together with: (i) the French University of Limoges [12];(ii) the Turkish Universities in Bartin and in Manisa [18]; and, (iii) the University West in Sweden [19].

References

1. T. Lampke, B. Wielage, H. Pokhmurska, C. Rupprecht, S. Schuberth, R. Drehmann, and F. Schreiber, Development of particle-reinforced nanostructured iron-based composite alloys for thermal spraying, Surf. Coat Technol., 205 (12) (2011) 3671-6.
2. T. Lindner, H. Liborius, B. Preuß, N. Hanisch, A. Schubert, and T. Lampke, Enhanced abrasion resistance of spark plasma sintered and HVOF sprayed Hadfield high manganese steel by turning and diamond smoothing, J. Manuf. Mater. Process, 6 (48) (2022).
3. S. Steinhäuser, B. Wielage, U. Hofmann, T. Schnick, A. Ilyuschenko, and T. Azarova, Plasma-sprayed wear-resistant coatings with respect to ecological aspects,Surf. Coat Technol., 131 (1-3) (2000) 365-71.
4. S. Tondu, T. Schnick, L. Pawlowski, B. Wielage, S. Steinhäuser, and L. Sabatier, Laser glazing of FeCr–TiC composite coatings, Surf. Coat Technol. 123 (2000) 247-51.
5. H. Podlesak, T. Schnick, L. Pawlowski, S. Steinhäuser, and B. Wielage, Microscopic study of Al–SiC particulate composites processed by laser shocks,Surf. Coat Technol. 123 (2000) 247-51.
6. B. Wielage, T.Grund, C. Rupprecht, and S.Kümmel, New method for producing power electronic circuit boards by cold-gas spraying and investigation of adhesion mechanisms, ibid. 205 (4) (2010) 1115-18.
7. D. Dietrich, B. Wielage, T. Lampke, and S. Kümmel, Evolution of microstructure of cold-spray aluminum coatings on Al2O3 substrates, Adv. Eng. Mater., 14 (4) (2012) 275-8.
8. R. Drehmann, T. Grund, T. Lampke, B. Wielage, K. Manygoats, T. Schucknecht, and D. Rafaja, Interface characterization and bonding mechanisms of cold gas-sprayed Al coatings on ceramic substrates, J. Thermal. Spray Technol., 24 (2014) 92-9.
9. P. Sokolowski, L. Pawłowski, D. Dietrich, T. Lampke, and D. Jech, Advanced microscopic study of suspension plasma-sprayed zirconia coatings with different microstructures, ibid., 25 (2016) 94-104.
10. P. Sokołowski, P. Nylen, R. Musalek, L. Łatka, S. Kozerski, D. Dietrich, T. Lampke, and L. Pawłowski, The microstructural studies of suspension plasma sprayed zirconia coatings with the use of high-energy plasma torches, Surf. Coat Technol., 318 (2017) 250-61.
11. Ali, D. Wett, T. Grund, and T. Lampke,TGO formation and failure mode of TBC systems comprising PVD-AlOx interlayers, Proc. ITSC, Shanghai, China, 1 (2016) 156-60.
12. Ali, P. Sokołowski, L. Pawłowski, D. Wett, T. Grund, and T. Lampke, Study on the characteristics of a TBC system containing a PVD-Al interlayer under isothermal loading, Coatings, 11 (8) (2021) 887.
13. T. Lindner, E. Saborowski, M. Scholze, B. Zillmann, and T. Lampke, Thermal spray coatings as an adhesion promoter in metal/FRP joints, Metals, 8 (10) (2018) 769.
14. E. Saborowski, P. Steinert, A. Dittes, T. Lindner, A. Schubert,and T. Lampke, Introducing fractal dimension for interlaminar shear and tensile strength assessment of mechanically interlocked polymer–metal interfaces, Materials, 13 (9) (2020) 2171.
15. M. Grimm, S. Conze, L.-M. Berger, G. Paczkowski, R. Drehmann, and T. Lampke,Changes in the coating composition due to APS process conditions for Al2O3-Cr2O3-TiO2 ternary powder blends, J. Thermal. Spray Technol., 3 (2021) 168-80.
16. M. Grimm, S. Conze, L.-M. Berger, G. Paczkowski, T. Lindner, and T. Lampke, Microstructure and sliding wear resistance of plasma sprayed Al2O3-Cr2O3-TiO2 ternary coatings from blends of single oxides, Coatings, 10 (1) (2020) 42.
17. F. Bocklisch, G. Paczkowski, S. Zimmermann, and T. Lampke, Integrating human cognition in cyber-physical systems: A multidimensional fuzzy pattern model with application to thermal spraying, J. Manuf. Systems, 63 (2022) 162-176.
18. Cahit Karaoglanli, T. Grund, A. Turk, and T. Lampke, A comparative study of oxidation kinetics and thermal cyclic performance of thermal barrier coatings (TBCs), Surf. Coat. Technol., 371 (2019) 47-67.
19. M. Ossiansson,M. Gupta, M. Löbel, T. Lindner, T. Lampke, and S. Joshi, Assessment of CrFeCoNi and AlCrFeCoNi high-entropy alloys as bond coats for thermal barrier coatings, J. Thermal. Spray Technol., 126 (2022).

Thermal Spray Coating, Reconceptualized

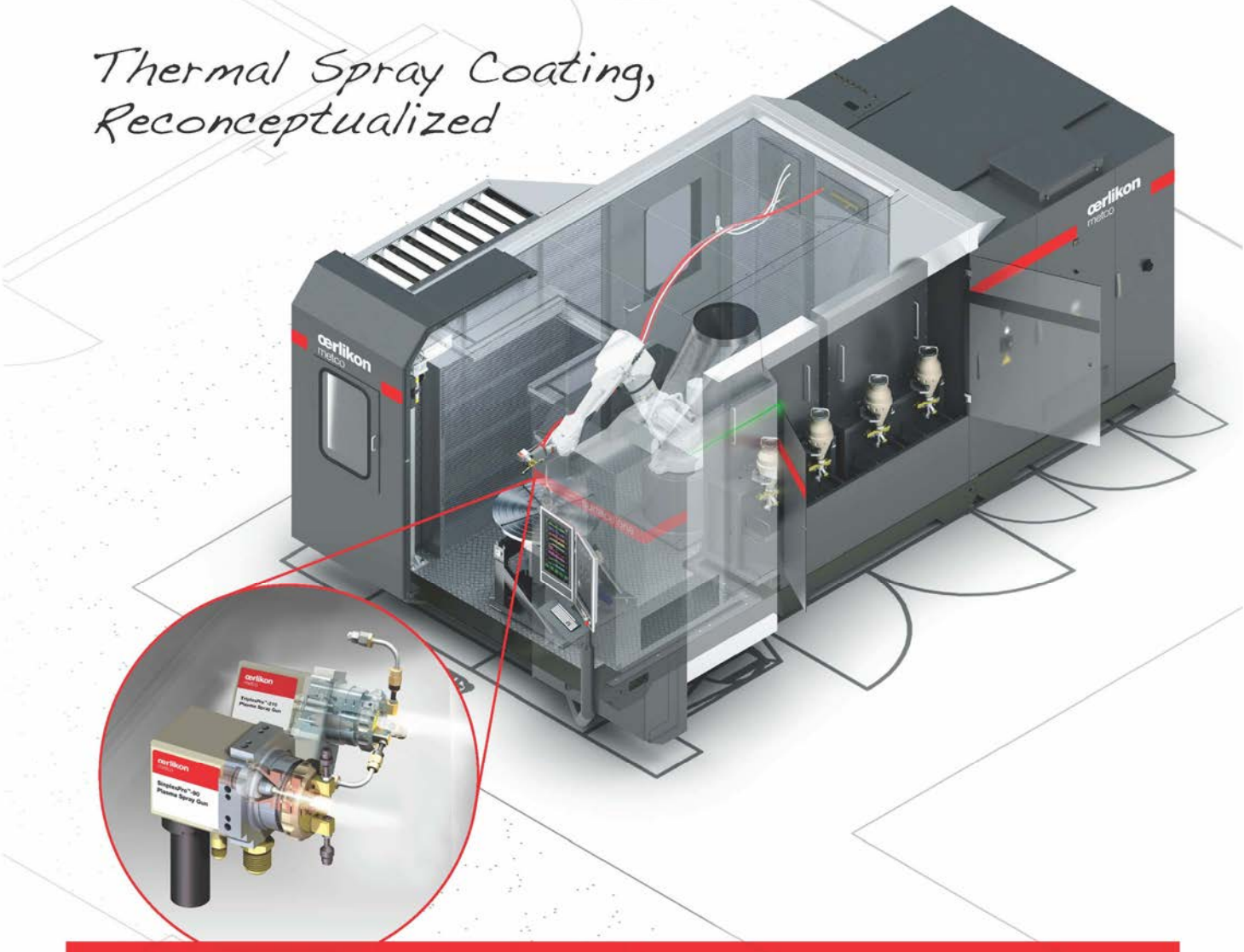

Surface One — The First Thermal Spray Coating Machine

We understand our customers' priorities and values — because we share them!
Like you, we strive to become more productive, adapt faster to changing market conditions and ensure the health and safety of our people. These objectives drove the reconceptualization of the thermal spray coating process and led to our launch of the first thermal spray coating machine: SurfaceOne™.

- Boost your productivity with improved usability and operator guidance
- Save floor space thanks to compact construction
- Benefit from increased flexibility to upgrade and relocate your production
- Protect your personnel and equipment with exceptional safety features

Pair Surface One with one of our versatile cascading arc plasma spray guns, SinplexPro™ or TriplexPro™, to produce high-performance coatings with workhorse durability and reliability.

www.oerlikon.com/metco

oerlikon
metco

Effect of Target Thickness on the TBC Deposition Characteristics and Microstructural Features

*By **Dr. Hugo Hernandez-Alvarez, Dr. Atin Sharma,** Siemens Energy Inc.5101 Westinghouse Blvd. Charlotte, NC. USA.*
Email: atin.sharma@siemens-energy.com

Introduction

Thermal Barrier Coatings (TBCs), manufactured via Atmospheric Plasma Spray (APS), have been used in gas turbines for decades. These coatings provide thermal protection to components located in the hot section of the engine (e.g., combustion transitions and baskets, blades, vanes, ring segments, etc.) [1, 2, 3].The components used in large power generation turbines are much larger and utilize much thicker coatings than their propulsion turbine counterparts. For some components, it could take several hours to apply coating and the manufacturing cost associate with, hardware and consumables is high. In production settings, design required target thickness for a given part is mostly achieved by adjusting the number of spray passes or increase feed rates [4]. Therefore, for a fixed component and a fixed set of spray parameters, a higher TBC thickness requires a higher number of spray passes. The underlying assumptions are that the coating thickness varies roughly linearly with the number of passes.

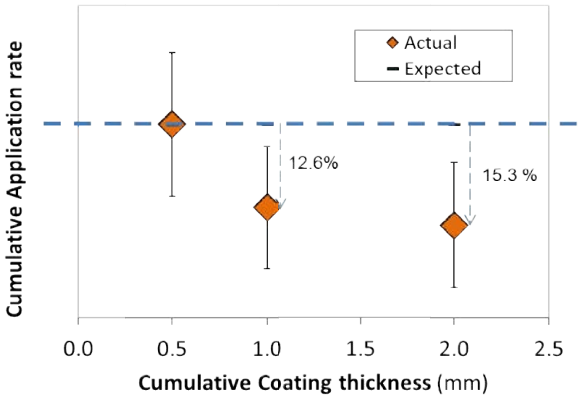

Figure 1: Change in coating application rate with thickness under actual production settings

In other words, the application rate remains constant independent of the target thickness. However, manufacturing data from roughly 200 pieces of a combustor part indicated that going from a 0.5 mm to 2.0 mm thick TBC (in the same spray run), there was a 15% drop-in application rate [5].

This prompted us to investigate (1) the causes governing this dependence of Application Rate (AR) on the TBC thickness and (2) whether it had any effects on the coating microstructure and properties.

Materials and Methods

Several TBCs samples were sprayed on stainless steel / mild steel using several spray parameter-sets. For each spray parameter set, two steel specimens with 25mm x20mm x5mm (for metallographic evaluation), and one mild steel plate 100 mm x100 mm x5 mm (for deposit efficiency (DE) and application rate (AR) evaluations) were prepared by grit blasting on one side, then cleaned with alcohol before spraying for APS deposition. A standard 150µmof CoNiCrAlY bond coat was applied prior to TBC application.

Commercially available 6-8wt%YSZ powders with Agglomerated& Sintered (A&S) and Fused & Crushed (F&C) morphologies were used for TBC top-coat. A range of spray parameters were applied to systematically vary the net enthalpy (heat input minus heat extraction) of the process. Table 1 shows the spray parameters used in this study. TBC thickness targets for this study were 0.5 and 2.0mm.

Table 1: Spray Parameters

Attribute	Value
Spray Process	APS
Spray torch	SM F4MB
Powder Composition	6-8 wt% YSZ
Substrate Type	Steel / Al
Gun power (kW)	33 - 44
Primary gas	Argon
Secondary gas	Hydrogen
Primary / Secondary flow ratio	3 – 5
Carrier Gas Type	Argon
Carrier Flow (SCFH)	10
Powder Feed Rate (g/min)	35 – 65
Spray Distance (inch)	4 – 6
Traverse Speed (mm/sec)	350 – 500
Sample / Part Cooling	Variable
Target Coating thickness (mm)	0.5 – 2.0

For DE evaluation, material was sprayed such that the coated area was smaller than the plate mild steel size (i.e., no spraying outside of the plate). Then the DE was calculated as follows:

$$Deposition\ Efficiency\ (DE) = \frac{Mass\ Deposited\ as\ Coating\ (g)}{Powder\ Feed\ Rate\ \left(\frac{g}{s}\right) \times time\ (s)}$$

Microstructural investigation was conducted on the stainless-steel samples by using optical microscope and SEM which included coating porosity, crack density and thickness etc. Coating Application Rate (thickness per pass) was determined from the metallographic coating thickness.

Results

Figure 2 (a) shows that the AR varies with target coating thickness and can increase or decrease with thickness depending on spray parameters used. On the other hand, the DE does not change with target coating thickness (Figure 2 (b)).DE measurements were performed only for the four of the six parameters used in this study.

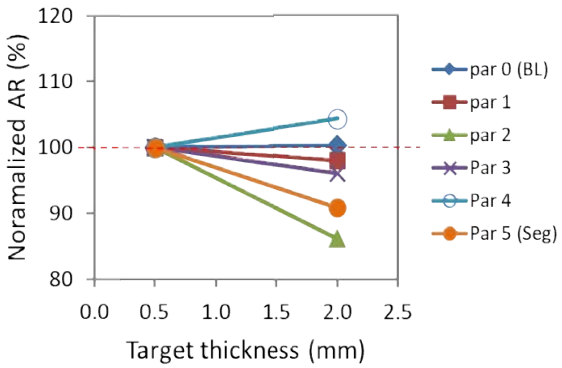

(a)

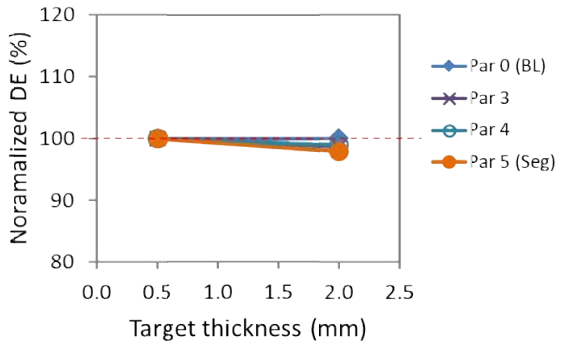

(b)

Figure 2: Change in the deposit characteristics with target coating thickness: (a) Application rate (AR) and (b) Deposit efficiency (DE)

Figure 3 presents the microstructures of TBC samples resulting from Parameter #0 (baseline parameter), Parameter #3, Parameters #4 and Parameter #5 at 0.5 mm and 2 mm thickness. The microstructures for Parameter #0 coatings are nearly independent of the target thickness. The porosities are homogeneously distributed and there are no exceptional features any target thickness. For Parameter #3 coating, the average coating porosity showed a decrease going from 0.5 mm to 2.0 mm. There are no vertical cracks (VCs)observed in the 0.5 mm coating sample but there are several vertical cracks in the 2.0 mm coating. The appearance of VCs was a remarkable finding which indicates increased levels of stresses in the TBC with higher thickness without any changes in the spray parameters. A similar observation was made with the 2.0 mm thick coating fabricated with Parameter #2 (microstructure not shown in this article) where VCs were observed in thicker version of the TBC. For Parameter #4 coating, the average coating porosity appears to slightly increase going from 0.5 mm to 2.0 mm. There are no other remarkable changes in the microstructural features of this coating with increasing thickness. For Parameter #5 (segmented) coating, the coating porosity did not show a discernible change going from 0.5 mm to 2.0 mm. The 0.5 mm and the 2.0 mm coatings show the crack density (number of vertical cracks per unit length). However, the VCs in 2.0 mm coating are wider and more pronounced.

TBC porosity measured via image analysis using optical microscope, is presented in Fig. 4. It is noted that the TBC porosity increases, decreases, or remains unchanged with coating thickness, depending upon the process parameters applied.

Parameter #	TBC microstructure at 0.5 mm target thickness	TBC microstructure at 2.0 mm target thickness
Parameter #0	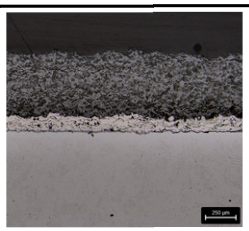	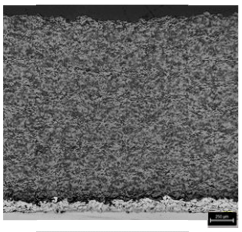
Parameter #3	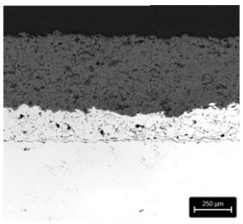	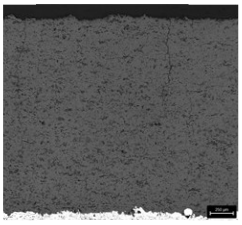
Parameter #4	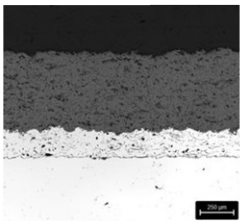	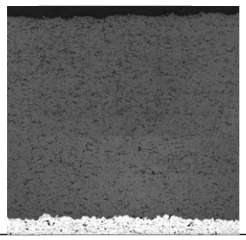
Parameter #5	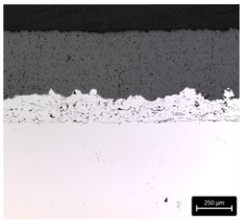	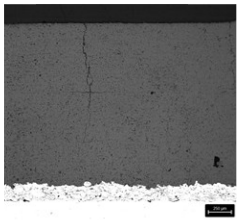

Figure 3: Microstructures of selected TBC samples at 0.5 mm and 2 mm thickness

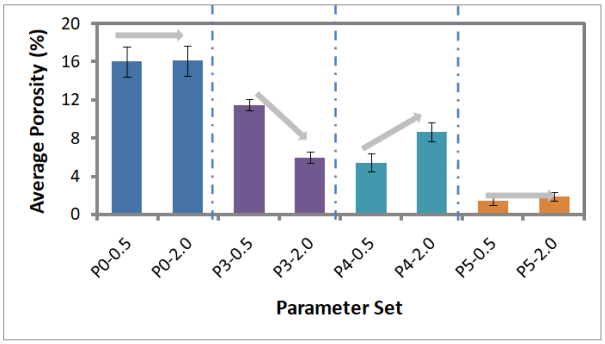

Figure 4: TBC porosity measured via image analysis using optical microscope

Discussion

The DE and AR are related as follows. By definition,

$$DE = \frac{Mass\ deposited\ as\ Coating}{Mass\ of\ powder\ fed}$$

$$= \frac{Coated\ area \times Application\ rate \times Caoting\ density}{powder\ feed\ rate} \quad (1)$$

Rearranging Equation (1), we get,

$$Coating\ Density = \frac{Powder\ feed\ rate \times Deposition\ Efficiency}{Coated\ Area\ \times Application\ Rate}$$

Since coating porosity is inversely proportional to coating density, we can write,

$$Coating\ Porosity \propto \frac{Coated\ Area \times Application\ Rate)}{Powder\ Feed\ Rate \times Deposition\ Efficiency} \quad (2)$$

This implies that if the powder feed rate, DE, and coated area are constant, then the coating porosity should be directly proportional to the AR. That is, under a constant feed rate, and a fixed coated surface area, if the AR decre

-ases going from 0.5 mm to 2.0 mm thickness, it can be expected that the 2.0 mm thick coating will have a lower porosity (or higher density) than the 0.5 mm thick coating, when there is negligible change in the DE between the two coatings.

- Examining Figure 2 in the light of relationship (2), the following predictions can be made
- The TBCs resulting from Parameter #0 (baseline parameter) would show nearly the same porosity in 0.5 mm and 2 mm thick samples
- The TBCs resulting from Parameters #3 and #5 would show a reduction in porosity in the 2 mm thick sample relative to the 0.5 mm thick ones
- The TBCs resulting from Parameters #4 would show an increase in porosity in the 2 mm thick coating relative to the 0.5 mm thick ones

TBC porosity in Figure 4 is indeed consistent with the above predictions in all cases except Parameter #5 (segmented TBC) where the porosity seems to slightly increase rather than decreasing (as per the prediction). Possible reasons behind this anomaly may be (1) the overall low porosity (<2%) of segmented TBC which does not leave much further scope for reduction in porosity via thermal spray process. The low porosity is also approaching the detection limit of optical microscopes making it difficult to discern small changes in porosity at that level (2) the wider crack opening in thicker (2 mm) segmented TBC may be counted toward porosity and may result in higher porosity number even though the actual porosity in the bulk of the TBC may have decreased.

Thus, it appears that the coating microstructure and AR can experience from negligible to significant changes in with thickness depending upon the process parameters. To explain the observed behavior, we propose the following hypothesis:

Each set of process parameters has a certain amount of heat input into the coating (depending upon the torch power, spray distance, powder feed rate, surface speed etc.) and a certain amount of heat extraction (depending front and back cooling air flow, coating, and substrate thickness etc.). The difference of heat input and heat extraction is defined as the net process enthalpy. As the coating becomes thicker, its thermal insulation increases which leads to an increase in the net process enthalpy for any given process. When the net process enthalpy becomes high enough with increased thickness, it leads to an improved flattening of powder particles and the inter-splat adhesion.

This in turn renders reduced porosity (increases density) of the coating and hence reduced AR as explained above. In some cases, the increased coating density and inter-splat adhesion can lead to higher stresses resulting in vertical segmentation. This is perhaps what happened to the thicker versions of TBC in Parameter #2, #3 and #5. The segmented TBC (Parameter #5) already had vertical segmentations even in the thinner version and the crack density did not increase with thickness, but cracks became more pronounced in the higher thicker thickness version.

On the other hand, for some processing conditions, the net process enthalpy may not change with increased coating thickness, or the net enthalpy may increase with increased coating thickness but the reduction in AR is compensated by the entrapment of unmolten particles. In such scenarios, either there would be no change, or slight increase in AR with thickness. This may have been the case with Parameter #0 and number #4. Figures 5 and 6 show the higher magnification SEM images of the thin (0.5 mm) and the thick (2.0 mm) versions of TBCs fabricated with Parameters #0 and #4, respectively.

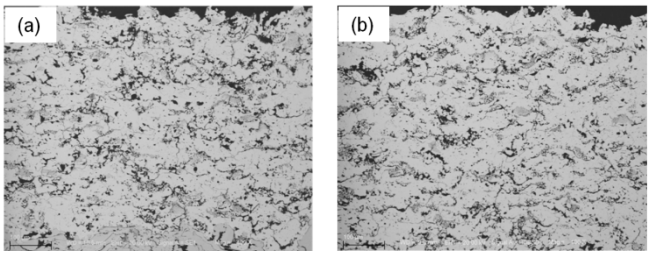

Figure 5: SEM images of Parameter #0 TBC at 400X: (a) 0.5 mm coating and (b) 2.0 mm coating

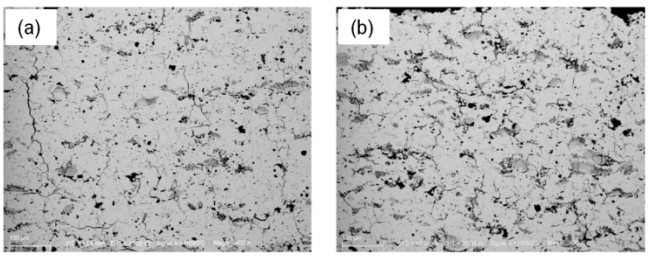

Figure 6: SEM images of Parameter #4 TBC at 400X: (a) 0.5 mm coating and (b) 2.0 mm coating

For parameter #0, the 0.5 mm coating and the 2.0 mm coating have similar areas with fine pores and entrapped unmolten powder particles. For parameter #4, the 2.0 mm coating has more areas with fine pores and entrapped unmolten powder particles than that in 0.5 mm coating. These micrographs provide evidence to support the proposed hypothesis.

Conclusions

In serial production of some gas turbine components, the TBC application rate was found to vary as a function of target thickness rather than staying constant. A systematic spray DoE study was performed to investigate this effect. The correlation between the coating deposit efficiency and application rates indicated the possible differences in coating microstructure between thin and thick coatings. Coating porosity investigated using optical microscope was consistent with the expected variation of coating porosity with thickness in all cases except the segmented TBC. There are other indications such as vertical micro-cracks in the coatings that provide hints about the possible underlying phenomena behind these effects. A plausible (preliminary) hypothesis describing the observed behavior was proposed which is supported by detailed SEM evaluation of the coatings. The correlation of the observed microstructural features with the physical properties such as coatings hardness, elastic modulus and thermal conductivity will be investigated in the future which may provide further insights into this "thickness" effect.

References

1. Clarke, D.R., Oechsner, M. &Padture, N.P. Thermal-barrier coatings for more efficient gas-turbine engines. MRS Bulletin 37, 891–898 (2012).
2. A.G. Evans, D.R. Clarke, C.G. Levi, Journal of the European Ceramic Society. 28, 1405 (2008).
3. Mondal, Kunal, Nuñez, Luis, Downey, Calvin M., and van Rooyen, Isabella J. Thermal Barrier Coatings Overview: Design, Manufacturing, and Applications in High-Temperature Industries. Idaho National Lab. Idaho Falls, ID (United States), (2021).
4. Lima, R.S. Porous APS YSZ TBC Manufactured at High Powder Feed Rate (100 g/min) and Deposition Efficiency (70%): Microstructure, Bond Strength and Thermal Gradients. J Therm Spray Tech 31, 396–414 (2022).
5. Hernandez-Alvarez, Hugo and Sharma, Atin. Effect of target thickness on the TBC application rate, microstructure and properties. ITSC 2018. May 7-10, 2018. Orlando, Florida USA.

To contribute an article, advertisement, subscription request, back issue copies, and changes of address should be sent to: todayspray@outlook.com and todayspray@gmail.com

PhD, Postdoc & Research Engineer Job Alerts

PhD position is available at **Networked Optimization, Diagnosis & Estimation (NODE) Lab and Advanced Heat Transfer and Surface Technologies Lab** (https://sites.ualberta.ca/~andre2/):
Interested candidates may send their questions or their CV, together with a cover letter and the names of three references to Dr. Ehsan Hashemi (he/him), ehashemi@ualberta.ca
Submission Deadline: July 11, 2022 or until the position is filled.
For more info please visit https://bit.ly/39BDDyC

PhD Scholarship available at the **Swinburne University of Technology (SUT - Australia)** ARC Training Centre in Surface Engineering for Advanced Materials (SEAM), led by Swinburne Distinguished Professor Chris Berndt (FASM, TSS Hall of Fame).
For more info please visit https://bit.ly/3OnKKK5

Research Scientists and Lead Engineer positions -GE (Niskayuna, NY, USA).
Research Scientist – Ceramics: Areas of focus include 3D printed ceramics for a wide variety of novel applications, ceramic matrix composites and environmental barrier coatings (CMCs and EBCs) for extreme environments, and functional ceramics for sensors and coatings. Apply today: https://invent.ge/3xXST2t

Lead Engineer – Coatings: in this role, you are expected to become a technical expert in a variety of thermal spray coating processes. Coatings include abradables, low-friction, wear, anti-corrosion, thermal barrier coatings (TBCs) and environmental barrier coatings (EBCs). Apply today: https://invent.ge/3xr5yJE

TBC Research Engineer - Blue Origin
Thermal and Environmental Barrier Coatings Research Engineer, Thermal Management Systems – Advanced Development Programs. Blue Origin (USA) is looking for an engineer with expertise in thermal barrier coatings (TBCs) and environmental barrier coatings (EBCs). For More Info please visit https://bit.ly/301L2GK

Process Engineering Manager- Coating and Joining Technologies
For more info please visit https://bit.ly/3HqZbL2

Product Engineer-Cincinnati Thermal Spray (CTS)
Cincinnati Thermal Spray (CTS) is hiring (USA); including a Product Engineer with Thermal Spray experience (preferred). For more info please visit https://www.cts-inc.net/about/careers/ or https://bit.ly/3QqkBf9

Sales representative- SPRAYWERX
SPRAYWERX (North Vancouver, BC, Canada) is hiring a thermal spray sales representative
For more info please visit https://bit.ly/3Qn8Bet

TATA STEEL
WeAlsoMakeTomorrow

TATA

Ceramat Private Limited, an initiative of New Materials Division, Tata Steel Limited.

Thermal Grade Hydroxyapatite for Implant Coatings

Product Technical Datasheet: **Hydroxyapatite Powder (>99%), synthetic**

PRODUCT DETAILS:

1. Introduction

Hydroxyapatite is naturally occurring biomineral of calcium apatite making 50 – 70% weight of human bone. TATA Synthetic hydroxyapatite powder is predominantly used to manufacture bone grafting materials, filling of bone defects, surface coating of biomedical implant and scaffolds fabrication (conventional/ additive manufacturing) for enhanced osseointegration. TATA-IISc Hydroxyapatite, BCP, β-TCP and the phase-pure metallic (Sr, Fe) derivatives of HAp pioneer in these fronts offering high chemical purity (assay >99.0%) and consistent spherical morphology to exceed the quality expectations in multifaceted biomedical and clinical applications. All our products are conformed with ISO and ASTM standards (ISO 13485, ISO 13779, ASTM F1185).

2. Salient Features

- Assured quality (conforming with international standards) with high purity (assay >99.0%).
- Wide varieties of products: Phase pure powder, doped powder, spray-dried powder
- Biomedical applications (implant coating)
- 'Make in India' and Unparalleled affordability

TECHNICAL DETAILS:

Classification	Synthetic bioceramics
Synonyms	Hydroxyapatite, HAp, Hydroxylapatite, Calcium hydrophosphate, Calcium phosphate hydroxide
Chemical formula	$Ca_5(PO_4)_3(OH)/Ca_{10}(PO_4)_6(OH)_2$
Formula weight	502.31 g/mol
CAS number	12167-74-7
Phase purity	X-Ray Diffraction, >99%
Ca/P ratio	1.66 – 1.8
Melting point	1100 °C
Decomposition Temp.	1670 °C (3038 °F)
Appearance	Pure white
Crystallite size	15-20 nm
Density (Gas pycnometry)	3.15 - 3.2 g/cc
Average particle size	≤ 1 µm
Spray dried powder	Spherical, D90 ≤30 µm
Coating route	Atmospheric plasma spray
International standards	ASTM F1185 ISO 13485-2016 and ISO 13779

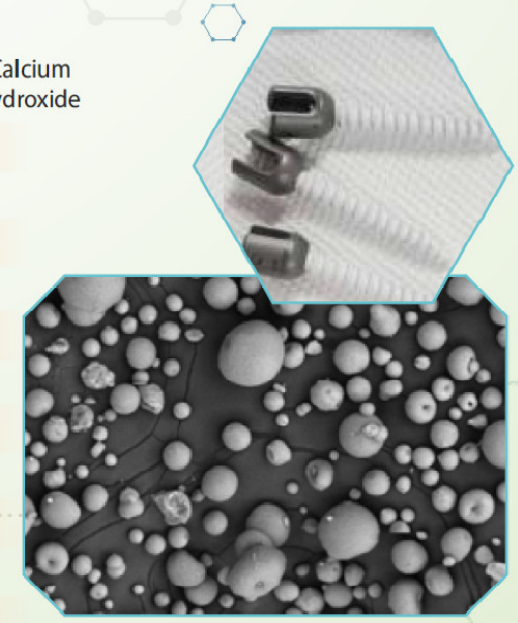

TATA HAp spray dried powder morphology

NEW MATERIALS BUSINESS
An Initiative of **Tata Steel**

For enquiries, please contact:
info@tsl-ceramat.com

3. PRODUCT INFORMATION

3.1 Chemical composition

Product	$Ca_5(PO_4)_3(OH)$ (wt%)	As (mg/kg)	Cd (mg/kg)	Hg (mg/kg)	Pb (mg/kg)	Total heavy metals	α-TCP (wt%)	β-TCP (wt%)	TTCP (wt%)	CaO (wt%)
Spray dried powder (code)	Balance	<3	<5	<5	<30	<30	<0.5	<0.5	<0.5	<0.5
Submicron powder (code)	Balance	<3	<5	<5	<30	<30	<0.5	<0.5	<0.5	<0.5

3.2 Particle size distribution, Grade and other features

Product	Particle size distribution	ASTM Grade	Production route	Morphology	Major applications
Spray dried powder (code)	40 – 500 microns (can be customised)	Medical	Wet precipitation> drying> slurry preparation> spray drying> calcination	Spherical	Plasma spray coating on biomedical implants
Submicron-powder (code)	20 – 200 nm	Medical	Wet precipitation> drying> calcination> sieving	Random	Biomedical implant, scaffolds fabrication

Upper particle size via sieve analysis is conformed with ASTM B214; lower particle size analysis using dynamic laser scattering (DLS)

3.3 Product selection guideline

- Spherical spray dried TATA HAp powder can be directly coated on the implant surface using atmospherical plasma spray coating process. This process does not need any bond coat and applies a rough and porous coating.
- Submicron size TATA HAp powder can be used in conventional/ additive manufacturing process to make patient specific scaffolds/ implants for bone salvaging application in case of segmental bone defect. Sterile slurry or spongy architectures can be fabricated bone void/gap filing or other applicable clinical interventions.

3.4 Related TATA products

- TATA products also covers an wide range of phase pure derivatives of Hydroxyapatite such as iron (Fe) and strontium (Sr) doped HAp. Phase pure β-TCP, biphasic calcium phosphate (BCP) with equal, higher or lower weight fraction of HAp rest balanced by β -TCP. Please contact TATA bioceramics product representative.

3.5 International Standards to be Referred

- Spray dried powder
- Submicron-powder
- ASTM F1185, EN: ISO 13485-2016 and ISO 13779-3

PUTATIVE APPLICATIONS:

- Biomedical implant coatings as thermal/plasma spray applications (dental, orthopaedic, trauma)
- Pharmaceuticals Calcium Phosphate products (tablets and emulsions)
- Scaffolds fabrication for hard tissue growth
- Grafts and Surgical blocks for bone and teeth
- Toothpaste and dental products

NEW MATERIALS BUSINESS
An Initiative of **Tata Steel**

For enquiries, please contact:
info@tsl-ceramat.com

A Novel Approach to Deposit Dense Cr_2O_3 Coating by Improved Flame Spray Process "H-LVOF"

*By **Dr. Satish Tailor, Ankur Modi**, Metallizing Equipment Company Pvt. Ltd., E-602-604, E.P.I.P. Boranada-342012, Jodhpur, India.*
Email: dgm_rnd@mecpl.com Web: www.mecpl.com

Abstract
Plasma sprayed Cr_2O_3 is widely used to protect industrial components against wear. This study presents an alternative improved flame spray process to deposit Cr_2O_3 coating having similar coating properties as like Plasma Sprayed ones. Recently, an advanced hybrid-low velocity oxy fuel (H-LVOF) method, trade name "CERAJET" has been considered as promising alternative to produce denser and more homogeneous ceramic coatings with lower as-sprayed surface roughness, similar or better coating properties compared to suspension plasma spraying, suspension HVOF and conventional APS-sprayed coatings. In this study, coatings were deposited without applying a bond coat and the microstructural, mechanical and wear properties of H-LVOF sprayed Cr_2O_3 coatings is presented. This study shows a non-expensive and simple method to produce dense Cr_2O_3 coating in large scale.

Introduction
There are numerous industrial applications of Plasma sprayed Cr_2O_3 coatings to provide protection against sliding and abrasive wear. A few examples are paper making rolls and blades, Anilox printing rolls, hydraulic seal joints, hydraulic rods and textile rolls, pump parts including rotors, shaft sleeves, seals, vanes and other wear parts, and components for high-speed automatic machinery, such as packaging and food processing machinery. Due to its excellent wear and corrosion resistance Cr_2O_3 is potentially suited to food-contact applications, protection of cylinder rings in internal combustion engines, sheet metal punching dies, ball valves and seats in hydrometallurgical applications. Pure Cr_2O_3 coatings are known to have outstanding sliding wear performance.

It was found that during the plasma spraying of Cr_2O_3 gaseous species (evaporation) are formed at high temperature [1-3], which reduces the deposition capacity (DE). Other ceramics such as TiO2 or Al2O3 are commonly used with Cr_2O_3 to control this evaporation [4-6]. Additionally, it was also reported that the formation of undesirable metallic Cr, CrO and Cr_3O_4 occurs in conventional APS process with reducing effect of argon/hydrogen plasmas, leading to a further reduction in the chromia phase [7-8].
In order to removing the problem of undesirable product formation during spraying of Cr_2O_3, low temperature gas fuel guns (flame spray and HVOF) could be a better option. Researchers are studying Cr_2O_3 suspensions in HVOF as well in order to deposit dense coatings. But it is observed that the every single pass can be seen in the microstructure, it can be attributed to the un-melted particles, vaporized dust of Cr_2O_3 and the formation of microporosity. This is likely to decrease the structural integrity of the coating. Due to excessive thermal loading from the relatively continuous passes and short spray distance, some vertical and horizontal cracks were also found which lead to coating failure and reduced coating properties [9-14]. It was also reported that for better coating performance and to avoid low deposition rates, high coating brittleness or the presence of metallic chromium and the possible formation of Cr(VI) during the thermal spraying process, need to add Al_2O_3 and TiO_2 contents with Cr_2O_3 [10].
On the other hand, thermal spray suspensions are more expensive than regular thermal spray grade powders. Further, very low DE is the problem with suspension thermal spraying. A Cr_2O_3 raw powder with particle sizes below 1 micron is used as feedstock; the deposition efficiency (DE) was between 12 and 18%. By applying an

$85Cr_2O_3/15TiO_2$ suspension, the DE could be increased up to 20% [13]. Therefore, using suspensions in thermal spraying could not be an economical solution.

The aim of this study is to develop a cheaper process to deposit quality ceramic coating of Cr_2O_3 as like suspension HVOF and suspension plasma spray process produces. Additionally, coating could be applied to a metal substrate without the need for a primary bond coat. The microstructural, mechanical and wear properties of H-LVOF sprayed Cr_2O_3 coating are investigated.

Material and methods

Coating Deposition and Characterizations

Recently, an advanced hybrid low velocity oxy fuel (H-LVOF) method, trade name "CERAJET" has been developed by M/s Metalizing Equipment Company Pvt. Ltd. Jodhpur, India; which can produce denser and more homogeneous ceramic coatings with lower as-sprayed surface roughness, similar or better coating properties compared to suspension plasma and suspension HVOF and conventional APS-sprayed coatings. High performance Al_2O_3 and Al_2O_3-TiO_2 coatings have been successfully deposited by H-LVOF. The concept and process of Hybrid-LVOF can be found elsewhere [15-16]. In addition, compared to plasma and HVOF, the flame radiation and the noise level are very low in H-LVOF process [15-16]. Further, APS produces a much brighter UV-C light and is very harmful for naked eyes which can lead to flash burn and eye damage; whereas, H-LVOF does not produce UV radiations. The H-LVOF process is a lower power consuming and economical process compared to the conventional APS process.

A robotic H-LVOF (Make-MECPL, India) was used to prepare the coating samples. Substrates were grit blasted with alumina grit and cleaned with ethanol. Surface roughness after blasting was 6±3 µm. The spraying parameters are listed in Table 1. The average coating thickness of 250 µm was deposited. A commercially available Cr_2O_3 powder (particle Size 10-45 Microns) feedstock was used to deposit the coatings. This choice of particle size and spray parameters is intended to allow sufficient melting to obtain a suitable coating. Low carbon steel plates of 50 x 50 x 5 mm3 were used as substrate material.

Microstructures were analyzed using a scanning electron microscopy (SEM: Carl Zeiss Evo18, Germany) equipped with an Oxford, EDS. As per ASTM B-276, an Image Analysis System (QSMIAS 4.0) was used to determine the porosity present in coatings. A Vickers micro hardness instrument (SHIMADZU HMV-G-21ST, Japan) was used to measure the microhardness of the coatings at the load of 300 g for all coatings. Ten readings were taken for each coating and an average value was calculated. Surface Roughness Tester (Mitutoyo Model- SJ-210, Japan) was used to measure the surface roughness of the as-sprayed coatings and readings were taken at five random locations. The adhesion strength was measured per ASTM C-633 using an Universal Testing Machine (Instron, USA). Fracture toughness of the coatings was also calculated using the Vickers indentation procedure. The expression KIC = 0.079 (P/a3/2) log (4.5a/c) was used in the fracture toughness calculation [13]. The average value was taken from ten readings. The SprayWatch (Osier, Finland) diagnostic system was used to measure the particle velocity and temperature of Cr_2O_3 powder during the spraying and found to be 226 m/s and 27970 C, respectively. Three-body dry abrasion tests were conducted as per ASTM-G65 to see wear characteristics of the coatings.

Table 1: H-LVOF parameters

Oxygen	50 slpm
Acetylene	65 slpm
Air	450 slpm
Powder feed rate	16 g/min
Carrier gas flow	12 slpm
Spray distance	70, 85, 100 mm
Spray angle	90°

Results and discussion

In general, conventional plasma sprayed and flame sprayed coatings have porosity level in the range of to 5-10%. Producing dense coatings by APS and flame are not possible. A typical plasma sprayed Cr_2O_3 coating microstructure is shown in Fig. 1a. HVOF sprayed suspension ceramic coatings are still not matured enough and still need a lot of research.

Figure 1(b,c,d) shows the cross sectioned microstructures of the H-LVOF sprayed Cr_2O_3 (45/10) coatings at different spray distances 70, 85 and 100 mm, at higher magnification. Influence of the spray distance can be seen clearly in the microstructures.

It can be seen that all three cases (at spray distances 70, 85 and 100 mm) produces dense coatings but at the spray distance of 100 mm, porosity level is very low as <1%, whereas at spray distance of 70mm and 85 mm, porosity level is found to be 3 % and 2%, respectively. As-sprayed coating (at spray distances 100 mm) had a low surface roughness Ra 1 ± 0.3 µm, and at 70 and 85 mm spray distance the Ra values are found to be Ra 1.3 ± 0.5 µm and Ra 2.1 ± 0.8, respectively.

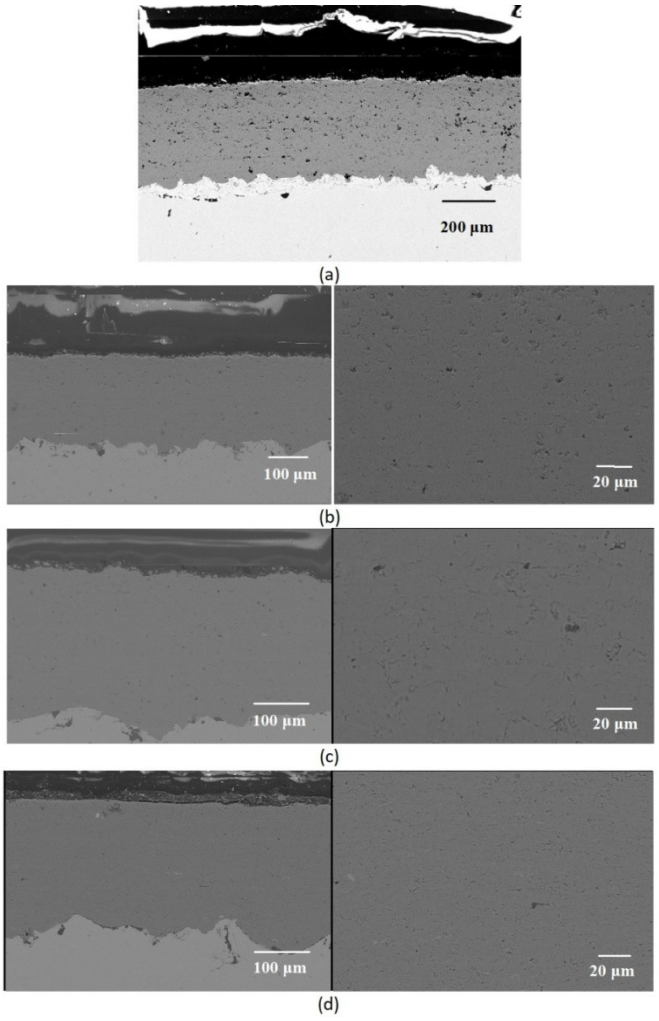

Figure 1: SEM micrographs of (a) Plasma sprayed coating, and H-LVOF sprayed coatings at different spray distances: (b) 70, (c) 85 and (d) 100 mm

A Vickers microhardness of 1373 ± 20 HV0.3, was found to be at 100 mm spray distance whereas 1250±25 HV0.3 and 1220±23 HV0.3 were found at 70 mm and 85 mm, respectively. Furthermore, a better fracture toughness of 0.8 ± 0.3 MPa_m0.5 was also observed at 100 mm spray distance. Without applying a bond coat, adhesion strength of the coating found to be 40±3 MPa. In comparison, plasma sprayed coating exhibit the hardness of 1150 ± 55 HV0.3, Adhesion strength 35±5 MPa and fracture toughness of 2±0.5 MPa_m0.5.

To examine wear characteristics of all as-sprayed coatings, three-body dry abrasion tests were conducted as per ASTM-G65. Alumina (80 meshes) was used as abrasive media with a fixed flow rate of 300 gm/min. Wheel rotation was set at 100 rpm. All coatings were tested at a load of 50 N for 200 cycles. H-LVOF sprayed coatings exhibits slightly better wear resistance than plasma sprayed coating (Fig. 2).

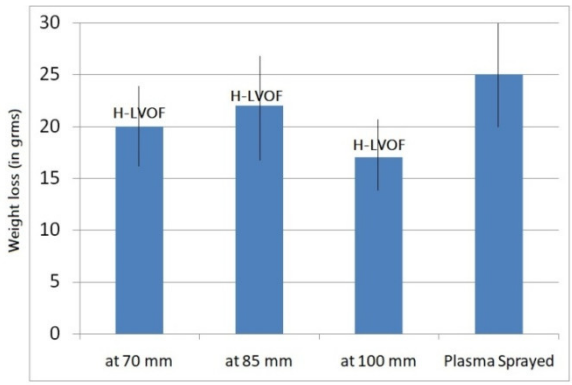

Figure 2: Weight loss in dry abrasion test

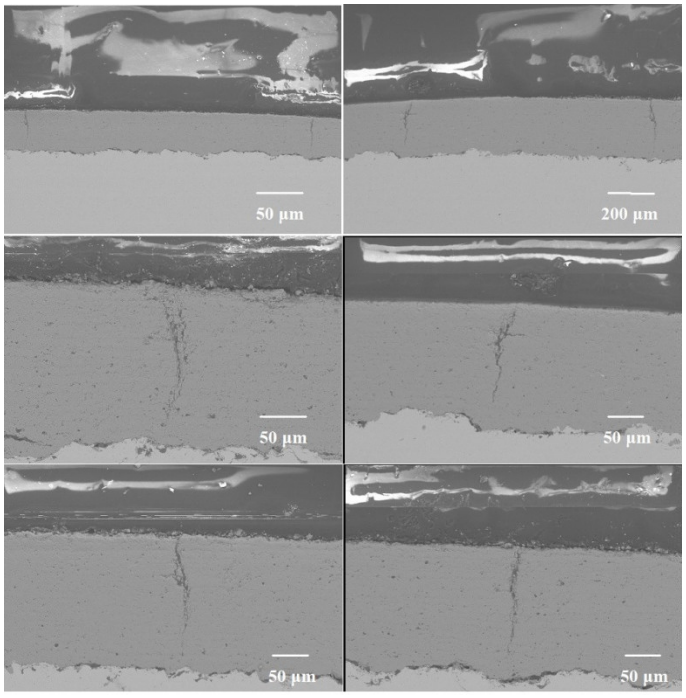

Figure 3: Cracks formation in the coating at different locations

Due to the relaxation of the residual stresses, forms a typical microcrack-like structure with high level of porosity (7-9 %) in the plasma sprayed coating (Fig 1a), which was not observed in the H-LVOF Cr_2O_3 coatings (Fig. 1b,c,d). Furthermore, due to the high temperature of the plasma flame, during spraying a bond coat is always required for plasma sprayed ceramic coating to compensate for the thermal mismatch between the substrate and the coating. Whereas, no bond coat is required in the H-LVOF process because the flame temperature is very low with respect to the plasma spray process. However, a bond coat is recommended for high temperature service conditions for greater durability and performance but where job service temperature is very low can be sprayed directly with H-LVOF process.

Sufficient cooling of the substrate is very important if no bold coat is applied. It was noticed that in absence of bond coat layer, continuous two passes of ceramic coat affect the coating properties and due to excessive thermal loading some vertical and horizontal cracks were formed inside the coating, as shown in Fig. 3. Whereas, controlled cooling of substrates eliminate this problem.

Conclusions

A process has been established to deposit dense Cr_2O_3 coating through H-LVOF process using available regular thermal spray grade commercial powder. H-LVOF is a cost effective method to produce ceramic coatings and could be an alternative of plasma spraying, suspension-HVOF and suspension plasma spraying (SPS) for ceramic coatings. The coatings show good mechanical and wear resistant properties, with no delamination at the coating/substrate interface while no bond coat was applied. In addition, coating properties are equal or better than plasma spraying and SPS. This will open gate for new application based on dense thin ceramic coatings.

References

1. D. Caplan and M. Cohen, The Volatilization of Chromium Oxide, J. Electrochem. Soc., 1961, 108(5), p 438-442.
2. G.R. Holcomb, Calculation of Reactive-Evaporation Rates of Chromia, Oxid. Met., 2008, 69(3–4), p 163-180.
3. P.L. Fauchais, J.V.R. Heberlein, and M.I. Boulos, Overview of Thermal Spray, Thermal Spray Fundamentals: From Powder to Part, P.L. Fauchais, J.V. Heberlein, and M.I. Boulos, Ed., Springer, New York, 2014, p 17-72.
4. L.-M. Berger, F.-L. Toma, S. Scheitz, R. Trache, and T. Börner, Thermisch Gespritzte Schichten Im System Al2O3–Cr_2O_3–TiO2 Ein Update, Materwiss. Werksttech., 2014, 45(6), p 465-475.
5. S.H. Yu and H. Wallar, Chromia Spray Powders. (United States), United States Patent and Trademark Office, 2006, p. 5.
6. L. Pawlowski, Technology of Thermally Sprayed Anilox Rolls: State of Art, Problems, and Perspectives, J. Therm. Spray Technol.,1996, 5(3), p 317-334.
7. M. Vippola, J. Vuorinen, P. Vuoristo, T. Lepistö, and T. Mäntylä, Thermal Analysis of Plasma Sprayed Oxide Coatings Sealed with Aluminium Phosphate, J. Eur. Ceram. Soc., 2002, 22(12), p 1937-1946.
8. Jarkko Kiilakoski, Richard Trache, Stefan Björklund, Shrikant Joshi, Petri Vuoristo, Process Parameter Impact on Suspension-HVOF-Sprayed Cr_2O_3 Coatings, J Therm Spray Tech (2019) 28:1933–1944.
9. Filofteia-Laura Toma, Annegret Potthoff, Maria Barbosa, Microstructural Characteristics and Performances of Cr_2O_3 and Cr_2O_3-15%TiO_2 S-HVOF Coatings Obtained from Water Based Suspensions, Journal of Thermal Spray Technology, 27, pages344–357 (2018).
10. A. Killinger, R. Gadow, G. Mauer, A. Guignard, R. Vaßen, and D. Sto¨ver, Review of New Developments in Suspension and Solution Precursor Thermal Spray Processes, J. Therm. Spray Technol., 2011, 20(4), p 677-695
11. J. Rauch, G. Bolelli, A. Killinger, R. Gadow, V. Cannillo, and L. Lusvarghi, Advances in High Velocity Suspension Flame Spraying (HVSFS), Surf. Coat. Technol., 2009, 203(15), p 2131- 2138.
12. A. Killinger, A. Rempp, A. Manzat, P. Mu¨ller, and R. Gadow, High-Velocity Oxy-fuel Spraying with Suspensions Consisting of Nanoscale and Submicronscale Oxide Powders, Therm. Spray Bull., 2015, 8(1), p 62-70
13. F.-L. Toma, S. Scheitz, R. Trache, S. Langner, C. Leyens, A. Potthoff, and K. Oerschla¨gel, Effect of Feedstock Characteristics and Operating Parameters on the Properties of Cr_2O_3 Coatings Prepared by Suspension-HVOF Spraying, in Proceedings International Thermal Spray Conference ITSC 2015 Long Beach, California USA, (ASM International, 2015), p 329-334.
14. Tailor, S., Vashishtha, N., Modi, A. et al. High-Performance Al_2O_3 Coating by Hybrid-LVOF (Low-Velocity Oxyfuel) Process. J Therm Spray Tech 29, 1134–1143 (2020).
15. Satish Tailor *et al*, Microstructure evolution and mechanical properties of Al_2O_3-40%TiO_2 coating by Hybrid-Low Velocity OxyFuel process, 2021 *Phys. Scr.* 96 025702.
16. Evans AG, Wilshaw TR. Quasi-Static Solid Particle Damage In Brittle Solids-I. Observations Analysis And Implications. ActaMetall 1976, 24: 939–956.

Structure-Property Correlation and High-Temperature Erosion Performance of Inconel625-Al_2O_3 Plasma-Sprayed Bimodal Composite Coatings

*By **Gaurav Prashar, Hitesh Vasudev**, Lovely Professional University, Phagwara, India-144411.*
Email: hitesh.24804@lpu.co.in

Introduction

A serious issue in the power plant and boiler industry is the degradation of a surface with solid particle erosion. The boiler tube faces regular failures, for which erosion and corrosion are the main diagnostic causes [1-4]. As the flue gases pass through the tubes of the boiler, erosion of the tube surface starts at various sections. It occurs primarily at tube side walls reducing its thickness and finally, the premature collapse of the tube occurs with time. Therefore, to enhance the efficiency and reliability of the boilers, detailed investigations must be done on the failed boiler tubes. Identifying and rectifying the leading cause of tube failures is vital to help to minimize the chances of future problems. A comprehensive assessment is the most effective method of determining the root cause of a failure. A tube failure is usually a symptom of other problems. A schematic outline indicating the actual region of a failure associated with boiler bed coils working at elevated temperatures inside an industry at Hoshiarpur, Punjab. India is shown in Fig.1. Damage has occurred on the impact side of the tube. Ultimate failure results from the rupture due to increasing strain as tube material erodes. It was concluded that failure of bed coils occurred due to thinning of bed coil (Fig.1b) from the outer diameter of the tube with time, caused by the abrasive nature of bed material ash which strikes the boiler bed coils with high velocity.

The metallic coatings on tubes minimize the degradation and erosion in the selected situations. To overcome this issue, materials that may have a combination of better mechanical and tribological properties need to be designed urgently. It can be reduced by employing surface modification methods like laser cladding, thermal spraying [5], weld overlays [6], heat treatments [7], etc. Because of its adaptability in depositing coatings of many types of materials, thermal spraying has been widely employed for the tailoring of component surfaces. These coatings extend the life of crucial components by minimizing the effect of wear and corrosion [8-11]. Plasma spraying is employed in various fields like aeronautics, astronautics, metallurgical, and petrochemicals due to its merits. The main advantages of plasma spray include precise composition and thickness control, unlimited substrate size and shape, cost efficiency, and bulk production capacity [12].

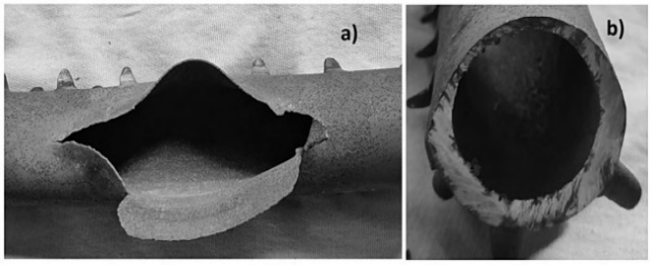

Figure 1: (a) Bursting of boiler bed coil tube, (b) thinning of wall tube due to erosion

The cermet coatings such as WC-Co-Cr, are well known for their effectiveness in protecting components against erosion. However, the expenses of producing these coatings are too high [14]. In general, nimonic (Ni-Cr) based coatings were suggested for components working at high temperatures. But their performance decline when service temperatures surpass 650 °C due to the diffusion of iron element into deposited coatings [15-18]. Due to this reason, there is a need to develop economical coating strategies to meet industry expectations.

Grewal et al., [20] reported that nickel powder blended with 40wt% Al_2O_3 reinforcement shows improved mechanical properties and good resistance to erosion in contrast with pure Ni. The influence of the Al_2O_3 addition on the mechanical properties of cold spray NiCr coating was examined. The improvement in wear resistance of cold spray NiCr coatings was observed [21]. Praveen et al., [18] also examined the addition of ceramic reinforcement (40wt%) Al_2O_3, in NiCrSiB matrix. The composite coating exhibited high erosion resistance and a significant increase in hardness owning to the reinforcement content. Dosta et al.,[22] also reported improvement in wear resistance of composite matrix with reinforcement of Al_2O_3 up to 30 wt% in IN625 matrix. Kim et al., [23] suggested that hard phase reinforcement content in ductile nickel matrix lies between 20 wt% to 40wt.%. In our previous study, the impact of reinforcing micrometric particles of Al_2O_3 (10, 20, and 30 wt.%) in the Inconel-718 matrix was analyzed. The highest erosion resistance was shown by coating with 30wt% Al_2O_3 (801 ± 40 Hv0.2) in comparison to 10 wt% and 20 wt% coatings, respectively. This was related to fact that the high content of Al_2O_3 increases the hardness of composite coating by restricting plastic deformation thereby improving erosion performance [19, 24-25]. Hence, composite coatings should be designed in such a manner that they will have the best possible merge of both hardness and toughness to combat erosive wear at elevated temperatures. But unfortunately, despite high hardness and improved tensile strength, composite coatings lack fracture toughness which is a principal property for resisting erosion failure [26]. Some studies available in the literature have also indicated the importance of bimodal coatings in enhancing mechanical properties [27]. The bimodal coatings developed from the combination of both micrometric and nanoparticles improve the erosion resistance at elevated temperature conditions.

In the present research study, an attempt has been put in to develop bimodal IN625-30%Al_2O_3 composite coatings and to compare them with micrometric and nanometric coatings. The novelty in the present work is the replacement of the available Ni and Ni-Cr nimonics matrix with the IN625 matrix. Moreover, to compare the effect of the addition of 30 wt% Al_2O_3 as reinforcement by varying the particle size in micrometric, nanometric, and bi-modal forms was also considered. In the current experimental study, the high-temperature erosion performance of plasma-sprayed coatings was studied. The micrometric, nano, and bimodal Al_2O_3 was reinforced with the IN625 matrix.

The composite coatings were deposited on ASTM SA210 GrA1 boiler steel. The substrate and coatings were evaluated at 900°C with a hot air-jet erosion tester at two angles. Nomenclature used and the composition of the different composite coatings developed using plasma spraying is highlighted in Table 1.

Table 1: Nomenclature and the composition of the different composite coatings developed using plasma spraying

Nomenclature	Matrix	Al_2O_3 size	Micro Al_2O_3 content %	Nano Al_2O_3 content %
IN625-ALC,	IN625	Micro	30	-
IN625-ALN	IN625	Nano	-	30
IN625-ALB	IN625	Micro + nano	15	15

The SEM-EDAX and XRD analysis were used for the microstructure characterizations of as-sprayed and eroded surfaces. The cross-sectional microstructures (low and high magnification) and XRD of as-sprayed coatings are shown in Fig.2 and Fig.3. As exhibited, all the plasma spray composite coatings were stacked tightly on the substrate with a coating thickness of around 250-300 µm. The magnified image of all the composite coatings shows a tightly packed lamellar structure and indicates that molten particles were compacted more effectively. The distribution patterns of micrometric-Al_2O_3 and nano-Al_2O_3 show considerable differences. The flattened splats can be seen in the IN625-AlC composite coating with micrometric reinforcement as shown in Fig 2b. The organic binder (PVA) used for agglomeration of nano-Al_2O_3 powders was burned during the deposition process in a plasma torch. The agglomerate nano-Al_2O_3 powder was dissociated, resulting in the creation of fine granules and splats in the IN625 matrix (Fig.2d). Some of the nano-Al_2O_3 particles were not melted sufficiently and retained in the IN625-ALN coating. In the IN625-ALB composite coating, the Al_2O_3 and flattened splats can be observed, with axes essentially parallel to the plane of the substrate. The same has better interfacial consistency with the IN625 matrix, pointing out that the added reinforcements are molten (Fig. 2f). The presence of a dark phase in all composite coatings indicates the Al_2O_3 hard phase, which was further confirmed by the EDS mapping of all three composite coatings not presented here.

Other researchers have documented the presence of Al_2O_3 in the microstructure in the form of a dark phase [20]. The presence of alumina at these locations was confirmed with X-ray maps also.

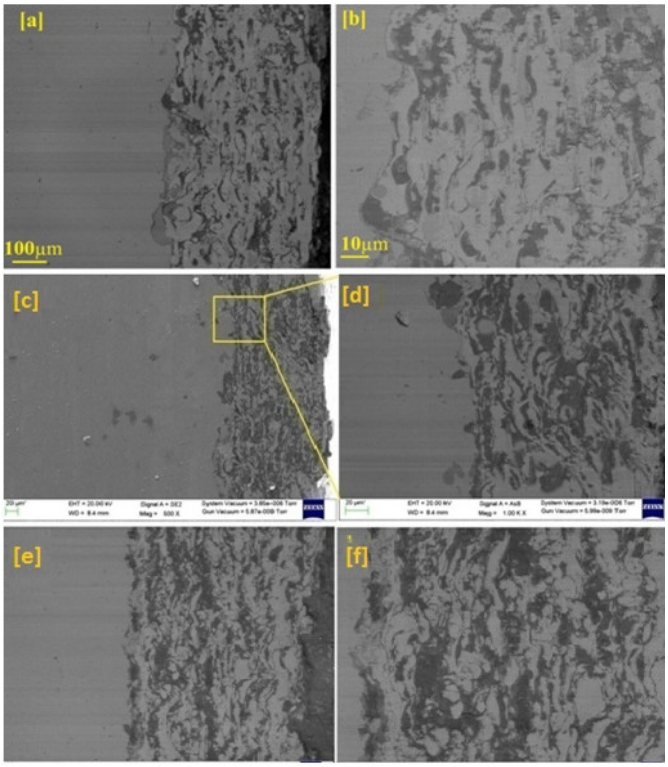

Figure 2: Cross-sectioned images of as-sprayed (a & b) IN625-ALC coating, (c & d) IN625-ALN coating, (e & f) IN625-ALB coating

The XRD results of plasma spray deposited IN625-ALC, IN625-ALN, and IN625-ALB composite coatings are presented in Fig.3. XRD analysis indicates peaks of Ni-Cr (FCC phase) in the IN625-ALC, IN625-ALN, and IN625-ALB composite coatings. A few low-intensity peaks of Cr_2O_3 were also observed in all deposited coatings. The XRD pattern of alumina (JCPDS reference no.00-001-1243) demonstrates the presence of the α-Al_2O_3 phase in the feedstock powder. It indicates that Al_2O_3 has maintained its identity even during the deposition of coatings. The Al2O3 in all coatings is corundum α-phase and this may be due to the following mentioned reasons. Firstly, the lower spraying velocity was achieved during plasma spray allowed for higher corundum content in the deposited coatings. This finding can be explained by the fact that the feedstock powder is fused in the hot flame of plasma during the deposition, resulting in the formation of γ-alumina. But γ-Al_2O_3 can be converted back to corundum α-phase as the granules in the deposited coatings cool more slowly owing to lesser spraying velocities. Secondly, due to shorter residence times at higher temperatures, part of the initial corundum α-phase has not converted to γ-alumina and was retained in the final deposited coatings, thereby maintaining the primary powder nanostructure. Finally, in the SEM micrographs, Al_2O_3 particles can also be seen in the un-melted form in the deposited coating. A portion of the low-weight agglomerated Al_2O_3 feedstock cannot reach the center of the spray flame. In this situation, a portion of the feedstock could not melt properly, resulting in the formation of the α-Al_2O_3 phase within the deposited coatings.

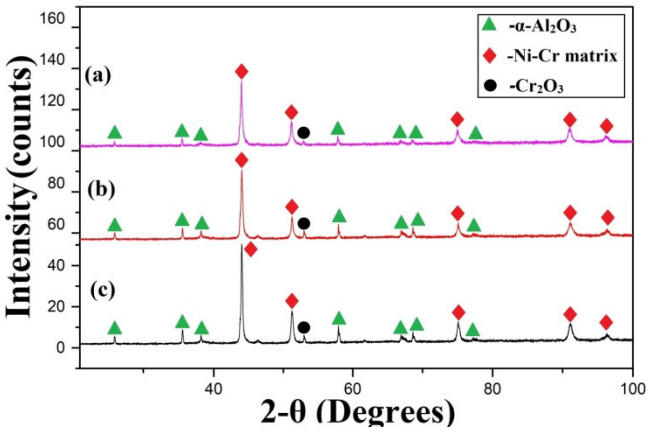

Figure 3: XRD patterns of the developed composite coatings: a) IN625-ALC, b) IN625-ALN and c) IN625-ALB

The SEM surface morphologies of IN625-ALC, IN625-ALN, and IN625-ALB coated samples at 30° and 90° impact angles are shown in Fig.4-6. The splat removal, cracks, and fracture are the major erosion mechanism responsible for material removal in coated samples. At an angle of 30°, the existence of sites indicates that material removal takes place by the medium of splats removal as shown in Fig.4(a) and 4(b), respectively. At oblique impact angle, tangential forces acting on splats owing to incoming erodent particles were high which results in detachment of splats [18]. IN625-ALC composite structure exhibited better erosive wear resistance at an angle of 30° in comparison to 90° impingement angle due to the shielding effect of blocky Al_2O_3 particles. Identical results were also observed in the literature previously. At glancing impingement, in the case of IN625-ALN (Fig.5a &b) and IN625-ALB (Fig.6a &b) composite coatings, the reinforcement of nano-Al_2O_3 enhances the cohesion of powder particles in contrast to the IN625-ALC coatings. The SEM micrographs of eroded IN625-ALN coating (Fig.5b&c) showed the existence of fractured Al_2O_3 splats, cracks, and detached splats.

The micrographs (Fig 4 c-d) of eroded surfaces indicate Al_2O_3 fractured splats, cracks, and removed splats as

the main erosion mechanism at a 90° impingement angle. At an impingement angle of 90°, the eroded IN625-ALN (Fig 5 c-d) and IN625-ALB (Fig 6 c-d) coating surfaces showed impressions of cutting produced by incoming eroded particles. However, in the case of IN625-ALC coating (Fig.4c-d), it experienced more material removal via cracking and spalling as compared to IN625-ALN and IN625-ALB coatings, respectively. This confirms identical findings by the studies of the erosive wear mechanism of Inconel718-Al_2O_3 coatings. At 90° impingement angle, all the composite coatings exhibited brittle erosion mode and detached finally from the surface of the coating with further impingements. In addition, at normal impacts Al_2O_3 particles shielding effect also reduces and dislocation accumulation in the frail bonding boundaries of alumina particles accelerates their pull-out. However, the nano-Al_2O_3 powder particles were evenly disseminated throughout the microstructure of the coating. Thus, they provide enhanced erosion resistance of IN625-ALN and IN625-ALB composite coatings at normal impact angles by providing dispersion strengthening.

IN625-ALB coated samples depict better erosive wear resistance among all the coatings at both testing angles. Because erosive wear resistance of the composite structure is a function of the material hardness and fracture toughness which controls the erosion behavior of coating. The fracture toughness and hardness value were more for the IN625-ALB composite coating followed by the other two coatings. Thus, an optimum mix of the hardness and toughness arising from the positive interaction among the micrometric and nano-Al_2O_3 particles helped in enhancing the erosion performance of IN625-ALB coated samples.

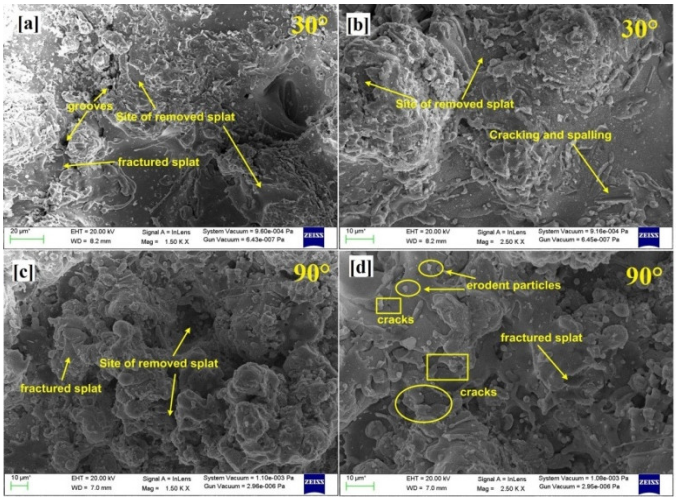

Figure 4: SEM images of: (a-b) eroded IN625-ALC coatings at 30° impingement angle and , (c-d) eroded IN625-ALC coatings at 90° impingement angle

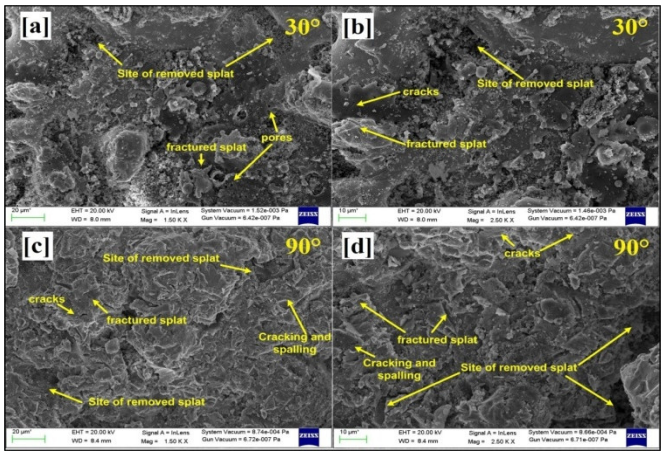

Figure 5: SEM images of: (a-b) eroded IN625-ALN coatings at 30° impingement angle and, (c-d) eroded IN625-ALN coatings C at 90° impingement angle

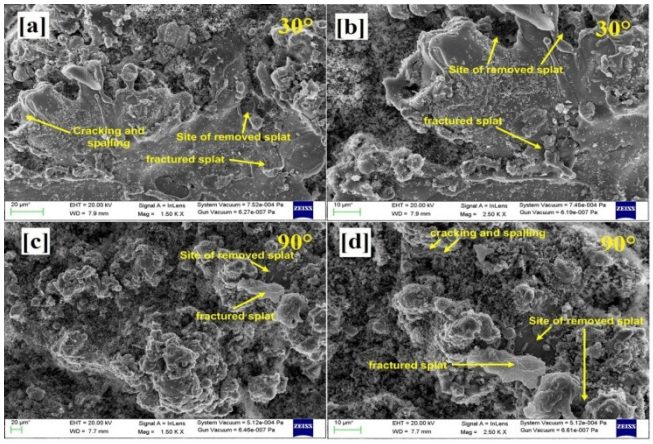

Figure 6: SEM images of: (a-b) eroded IN625-ALB coatings at 30° impingement angle and , (c-d) eroded IN625-ALB coatings C at 90° impingement angle

Results

Micro-hardness – Porosity – Fracture toughness - High temperature erosion test

Coating	Micro-hardness $H_{V0.3}$	Porosity%	Fracture toughness MPa√m	Erosive wear rate [g/g] at 30°	Erosive wear rate [g/g] at 90°
IN625-ALC	680±27	2.5	3.7	$4.7*10^{-4}$	$4.9*10^{-4}$
IN625-ALN	960±30	1.9	3.5	$4.0*10^{-4}$	$3.0*10^{-4}$
IN625-ALB	1130±25	1.5	5.2	$2.5*10^{-4}$	$2.1*10^{-4}$

The existence of grooves and lips at 30° and 90 ° impingement angles on surfaces indicate the erosion mechanism consists of ploughing and micro-cutting action for the substrate. All composite coatings exhibited brittle erosion mode. The detached splats, fracture, and cracks were the responsible mechanism of erosion in coatings at 30° and 90° impingement angles.

The erosive wear resistance of IN625-ALB composite coating improves approximately 4.57 times and 3.9 times in comparison with bare ASTM SA210 GrA1 at 30° and 90° impact angles respectively. The outcomes of the tests revealed that the bimodal composite coatings successfully protect the underlying substrate owing to their hardness and fracture toughness which is higher than the other two coatings. The better outcome of bimodal coatings was related to refined microstructures and good interaction among nano and micrometric Al_2O_3 reinforcement.

References

1. A. Kumar, and P.K. Sapra, Tribological characterisation of SA210 Gr A1 boiler steels for different temperature applications, Int. J. Surf. Sci. Eng, 10(4) (2016) 375-388.
2. M. Roy, Elevated temperature erosive wear of metallic materials, J. Phys. D: Appl. Phys. 39(6) (2006) R101.
3. A. Husain, and K. Habib, Investigation of tubing failure of super-heater boiler from Kuwait Desalination Electrical Power Plant, Desalination, 183(1-3) (2005) 203-208.
4. M.H. Mohamed, and V.H. Wilson, Analysis of boiler super heater tubes from high flue gas temperature, Int. J. Innov. Res. Adv. En. (2) (2015) 1-4.
5. J.C. Pereira, J.C. Zambrano, M.J. Tobar, A. Yañez, V. Amigó, High temperature oxidation behavior of laser cladding MCrAlY coatings on austenitic stainless steel, Surf. Coat. Technol. (270) (2015) 243-248.
6. E.M. Zahrani, and A.M. Alfantazi, High temperature corrosion and electrochemical behavior of INCONEL 625 weld overlay in $PbSO_4$-$Pb3O_4$-$PbCl_2$-CdO-ZnO molten salt medium, Corros. Sci. 85 (2014) 60-76.
7. G. Prashar, H. Vasudev, L. Thakur, Influence of heat treatment on surface properties of HVOF deposited WC and Ni-based powder coatings: A review, *Surf. Topogr.: Metrol. Prop.* (9) 043002.
8. L. Pawlowski, The science and engineering of thermal spray coatings, 2nd ed., John Wiley & Sons Ltd, London, 2008.
9. P.L. Fauchais, J.V. Heberlein, M.I. Boulos, Thermal spray fundamentals: from powder to part. Springer, 2014.
10. V.H. Hidalgo, J.B. Varela, A.C. Menendez, S.P. Martinez, High temperature erosion wear of flame and plasma-sprayed nickel-chromium coatings under simulated coal fired boiler atmospheres, Wear 247 (2001) 214-222.
11. J.R. Davis, Handbook of Thermal Spray Technology, 2nd ed, ASM International, USA, 2004.
12. G. Prashar, and H. Vasudev, Surface topology analysis of plasma sprayed Inconel625-Al_2O_3 composite coating, Mater. Today: Proc. 50(5) (2022) 607-611.
13. A. Anupam, R.S. Kottada, S. Kashyap, A. Meghwal, B.S. Murty, C.C. Berndt, A.S.M. Ang, Understanding the microstructural evolution of high entropy alloy coatings manufactured by atmospheric plasma spray processing, Appl. Surf. Sci. (505) (2020) 144117.
14. G. Prashar, H. Vasudev, L. Thakur, Performance of different coating materials against slurry erosion failure in hydrodynamic turbines: A review, Eng. Fail. Anal. (115) (2020) 104622.
15. T. Sundararajan, S. Kuroda, F. Abe, Steam Oxidation of 80Ni-20Cr High-Velocity Oxyfuel Coatings on 9Cr-1Mo Steel: Diffusion-Induced Phase Transformations in the Substrate Adjacent to the Coating, METALL. MATER TRANS A. 36 (2005), pp. 2165–2174.
16. Z. Yin, S. Tao, X. Zhou, C. Ding, Tribological properties of plasma sprayed Al/Al_2O_3 composite coatings, Wear, 263(7-12) (2007) 1430-1437.
17. N. Ramanujam, and T. Nakamura, Erosion mechanisms of thermally sprayed coatings with multiple phases, Surf. Coat. Technol. 204(1-2) (2009) 42-53.
18. A.S. Praveen, J. Sarangan, S. Suresh, J.S. Subramanian, Erosion wear behaviour of plasma sprayed NiCrSiB/Al_2O_3 composite coating, Int. J. Refract. Hard Met., 52 (2015) 209–218.
19. H. Vasudev, L. Thakur, H. Singh, A. Bansal, Effect of addition of Al_2O_3 on the high-temperature solid particle erosion behaviour of HVOF sprayed Inconel-718 coatings, Mater. Today Commun. 30 (2022) 103017.
20. H.S. Grewal, H. Singh, A. Agrawal, Microstructural and mechanical characterization of thermal sprayed nickel-alumina composite coatings, Surf. Coat. Technol. 216 (2013) 78–92.
21. H. Koivuluoto, P. Vuoristo, Effect of ceramic particles on properties of cold-sprayed Ni-20Cr+Al_2O_3 coatings, J. Therm. Spray Technol. 18(4) (2009) 555-562.
22. S. Dosta, N. Cinca, A. Silvello, I.G. Cano, Alumina Reinforcement of Inconel 625 Coatings by Cold Gas Spraying, Metals, 10(9) (2020) 1263.
23. H.J. Kim, S.Y. Hwang, C.H. Lee, P. Juvanon, Assessment of wear performance of flame sprayed and fused Ni-based coatings, Surf. Coat. Technol. 172(2-3) (2003) 262-269.
24. H. Vasudev, L. Thakur, H. Singh, A. Bansal, Erosion behaviour of HVOF sprayed Alloy718-nano Al_2O_3 composite coatings on grey cast iron at elevated temperature conditions, *Surf. Topogr.: Metrol. Prop.* 9(3) (2021) 035022.
25. H. Vasudev, G. Prashar, L. Thakur, A. Bansal, Microstructural characterization and electrochemical corrosion behaviour of HVOF sprayed Alloy718-nanoAl_2O_3 composite coatings, *Surf. Topogr.: Metrol. Prop.* 9(3), (2021) 035003.
26. A. Babu, H.S. Arora, H. Singh, H.S. Grewal, Microwave synthesized composite claddings with enhanced cavitation erosion resistance, Wear, 422 (2019) 242-251.
27. A. Babu, H.S. Arora, S.N. Behera, M. Sharma, H.S. Grewal, Towards highly durable bimodal composite claddings using microwave processing, Surf. Coat. Technol. 349 (2018) 655-666.

Thermal Spray Energy Efficiency Calculations

*By **Purusottam Sahoo,** Materials Solutions International Sugar Land, Texas – USA.*
Email: psahoo0077@gmail.com

At an ITSC conference many years in Long Beach, California, I had the pleasure of meeting with and talking to several "youngsters" involved in our industry. As a "second" generation thermal spray coating experimentalist, it appeared to me that we have come full-circle in some instances and are asking the same questions we queried our "seniors" when I was first starting out in this business. As someone who has been involved in coating gas turbine components, primarily to enable higher operating temperatures (and, thereby, increase the operating efficiency of the engine), it is somewhat ironic that our primary mode of applying such a coating is so very inefficient! Allow me to explain:

> Work and Energy are the same and is measured in Joules (J).
> Heat is the same as energy (really, the concept of "quantity of heat" has meaning in the context of an interaction where energy is transferred from one system to another as a result of a temperature difference), and has the same units as energy or work
> Power is the rate at which work is done, and is measured in Watt (W) = J/sec
> 1 hp ~750 W

This article was written many years ago for a private audience and it seems to me that it perhaps can explain my aforementioned statement about the process inefficiency.

As an example, let's calculate the amount of heat required to melt thermal spray powders and the resulting melting efficiency.

For matters of simplicity, let's take the case of plasma spraying. The power generated Q is equal to the voltage times the amperage. Thus

$$Q = I \times V \qquad (1)$$

If we take typical spray parameters for a CoNiCrAlY powder, the nominal voltage and amperage are 74 and 500 (assuming a Metco-Oerlikon 3MB plasma gun), respectively, at the spray control console. Typically, the gun voltage is a few V lower. In this case, assume the gun voltage is 70V

Thus, by equation (1)

$$Q = 500\ A \times 70V = 35000\ watts = 35000\ J/s$$
$$= 35000/\ 4.184\ cal/s = 35\ kW \qquad (2)$$

The heat required to heat any material to some final temperature T_f (which may include a change of state, e.g. melting, evaporation, etc.) is given by:

$$\Delta H = \int_{298}^{T} C_{p(s)}\,dT + \Delta H_f^T + \int_{T}^{T_f} C_{p(l)}\,dT \qquad (3)$$

The above equation represents: melt solid at a temperature T that is below T_f, and then to heat the liquid to T_f, where

Cp (i) is the specific heat in the state (i) [s = solid, l=liquid]. The specific heat Cp is usually a polynomial function of temperature. For the sake of simplicity, we will assume Cp is a constant over the temperature range of concern.

Going back to our CoNiCrAlY (assume, Co-32Ni-21Cr-8Al-.5Y composition) example, since an alloy does not have a fixed melting point, we will use the range of 1,250° C. and 2,350° C (1523 -2623 °K, or an average of 2073 °K)- for the purpose of calculation.

Our powder feed rate, in spray parameter 21.3, is

$$5.5\ lbs./hr = 0.693\ g/s \qquad (4)$$

Assume the following:

Specific heat of powder is: 0.44 J/(g°K)

The specific heat/mole of all metals are ~ 25 J/(mole°K)

In 100 g mix, the g. moles of each is as shown in Table below, along with the calculations using the law of mixture rule, the specific heat is:

$$C_p = \frac{25x(0.653 + 0.545 + 0.404 - 0.297 + 0.006)}{100} = 0.476\,\frac{J}{gK}$$

The heat of transformation (fusion) for the metals are as shown: Using the rule of mixtures on the molar ratios, the average approximate heat of fusion is about 247 J/g

Heat of Vaporization of all the elements in the Periodic Table								
Element	Element	Element	Element					
Atomic Number	Symbol	Name	Heat of Vaporization		At. Wt	Composition, wt%	Moles	Heat of Vap.
13	Al	Aluminium	293 kJ/mol	293	26.98	8	0.296515938	86.87916976
24	Cr	Chromium	339 kJ/mol	339	51.996	21	0.403877221	136.914378
27	Co	Cobalt	375 kJ/mol	375	58.932	38.5	0.653295323	244.9857463
28	Ni	Nickel	378 kJ/mol	378	58.693	32	0.545209821	206.0893122
39	Y	Yttrium	380 kJ/mol	380	88.906	0.5	0.005623917	2.13708861
38.5Co-32Ni-21Cr-8Al-.5Y composition						Total moles =	1.90452222	677.0056949
Heat of vaporization =	6770.056949	J/g						

Thus, for a feed rate of 0.693 g/s, our power usage for melting is

171.4 J/s (5)

Let's also assume that about 1% of the metal is being vaporized. The heat of vaporization is shown in Table above.

Using the molar ratio of this MCrAlY powder, the approximate heat of vaporization is

6770 J/g (6)

In order to maintain simplicity, let us also assume that we are heating the powder just up to the melting point, with 1% being vaporized. This implies that the third term in eqn. (3) can be set to zero. Thus, the heat required to melt and spray the powder is

$$\Delta H = (C_p \Delta T + \Delta H_f + \Delta H_v)m \quad (10)$$

= (0.476 (2073-298) +171.4+6770x0.01) 0.693 J/s
= (844.9 +171+67.7) *0.693
= 750.9 J/s (11)

Heat Loss to water:

Heat loss to water is given by

$$\Delta H = mC_p\Delta T$$

Let's assume that water is flowing at 4 gallons/min (=4x3.785 l/min = 0.252 l/s = 252.3 ml/s)

Also, let's assume the water temperature rise is 30°F (=17°K).

The specific heat of water is about 4.2 J/g°K

thus, heat extracted by water per second is (1 ml of water = 1g mass)

252.3 x 4.2 x 17 = 18014 J/s (12)

Thus, of the 35KW power produced in the plasma torch, about 18KW are lost to cooling water; about 0.75KW is used to melt the powder. The rest is used to raise the temperature of the ionized gases, generate kinetic energy of the powder particles; the remainder is lost as light, sound, and resistance loss in the copper cables.

Trivia Tid Bits:
Energy required to bring a cup of water to boiling is ~ 75000 J.
Food calories are actually Kilocalories (i.e. if a slice of bread is listed as having 50 calories, it actually contains 50000 calories)!
½ lb. cheese has ~ 4000KJ. In order to get rid of all this energy (as in not gaining weight) one has to perspire 1.6 Kg of water!
Energy required to lift a 10 lb powder bottle 4" above rest takes 4.5 J

The specific heat of gases generally increases with temperature and pressure. Let's take the example of N_2: we can approximate (between room temp. and 1500°C, and @ 2 atm. pressure), the specific heat to be 0.26 cal/(g°K).

If our flow rate of nitrogen is ~ 150 scfh @ STP, the mass flow = 1.47 g/s. To heat up the gas to, say 10,000K, the power requirements are: ~ 16000 J/s (This is very much simplified, which disregards the ionization energy, heat liberated when the ions come to ground state from their excited state, etc.)

Kinetic Energy Calculations: Assume the powder particles have an uniform speed of 500 ft. per second = 15240 cm/s = 152.4 m/s At the feed rate being used, the KE is:

KE= ½ mv2 = 0.5 x 0.693/1000 x 152.4^2 = 8 J.

1 J = 1 kg m^2 s^{-2}

Thus, power expended in accelerating the particles to the terminal speed is ~ 8J/s.

Thus, more than 50% of energy is lost to water, about 2.4% is used to melt powder, most of the remainder in heating the gases, and the rest is lost as light, sound, I^2R loss. If we approximate the light to be that of a 100W bulb, the loss from light is 100J/s.

Trivia Tid Bits:
The average power of a loud shout is ~ 0.03W. A conversation generates 10-5W. The entire New York City population of about 10 million, if they were speak all at once, will generate an acoustical power of about 100W, enough to power one light bulb!
Trivia question: Which organ, your eye or your ear, is the more sensitive one?

To summarize:

Item	Energy, J/s (1 J/s=1W)	
Plasma torch	35000	JP=235KW; JK=75KW
Melting C1062 powder at 5.5 lbs./hr	900	Raising temperature to melting point; vaporizing 1% of powder.
Kinetic energy per second	10	
Energy loss to cooling water	18000	4 gal/min, 30oF delta T

For HVOF systems, since powders are mostly in the plastic or semi-molten state, the energy utilization efficiency for melting is much lower.

Homework questions:

1. Determine heat loss to water and energy utilized for Inconel type powders for the JK and JP.
2. Which of the several thermal spry processes is the most energy efficient process for spraying powders?

We invite you to join iTSA!

Why become a member of iTSA?

The iTSA provides the useful information to all colleagues interested in thermal spraying in the large industries, societies, job shops, university and laboratories. The iTSA members have access to the additional services such as job proposition, information about services related to thermal spraying in different states of India, forum of users which enables research of missing information related to thermal spraying and much more. The iTSA membership enables also a reduction in the fees of the events organized by the Society.

For more information please visit https://www.indtsa.org/ or write us info@indtsa.org

Our Journal Publication

Journal of Thermal Spray and Engineering (JTSE) ISSN: 2582-1474

JTSE is an international archival journal publishing scientific papers on thermal spray technology; Journal provides a platform for researchers to share their original and innovative findings, in addition to identifying methods of production and application that include, but are not limited to, HOVF, plasma spray, flame spray, wire arc spray, and cold spray, Powder technology, Gas flow, particle motion, and heat transfer, Stress and strain analysis, Coating deposition mechanism, Single particle deposition and solidification upon impact, Coating mechanical and thermal properties, Coating microstructures and phase transformation, Functional coatings, Torch design and optimization, New thermal spray technology, Robotic programming and kinematic analysis, Torch trajectory definition and optimization, Novel applications of thermal spray coating, Mathematical and theoretical analysis on related subjects, Finite Element Analysis on related subjects. JTSE Covers Review Articles, Research Articles, Letter To Editor, Conference & Book Review, Notes and Short Communications. All the published articles are available for Download for Free.

DOI: https://doi.org/10.52687/2582-1474/
Journal website http://www.inscience.in/JTSE.html
Manuscript Submission http://www.inscience.in/manuscript-submission.html

India's 1st thermal spray magazine…

iTSA®

Indian Thermal Spray Association

https://www.indtsa.org/

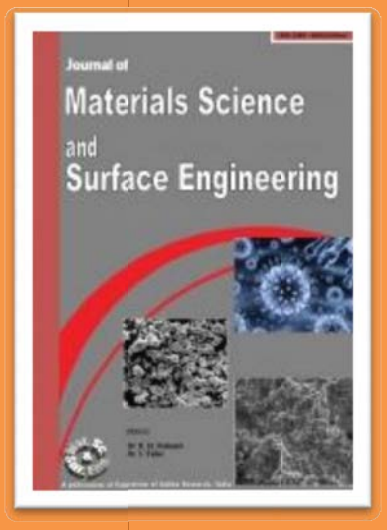

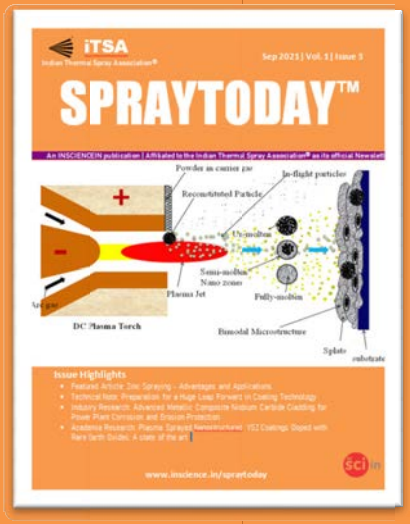

inSCIin

http://www.inscience.in/